

Review

Rheological Phase Reaction (RPR) as an Industrial Method for the Production of High Quality Metal Oxides towards Battery Applications

S. Pavithra ¹, A. Sakunthala ^{1,*} and M. V. Venkatasamy Reddy ^{2,*}

¹ Solid State Ionics Lab, Department of Applied Physics, Karunya Institute of Technology and Sciences, Coimbatore 641 114, Tamil Nadu, India

² Nouveau Monde Graphite (NMG), Saint-Michel-des-Saints, QC J0K 3B0, Canada

* Correspondence: sakunthala@karunya.edu (A.S.); reddymvvr@gmail.com (M.V.V.R.)

Abstract: Although research on the preparation of metal oxides and other materials for various applications increases exponentially, it is more important to understand the need for eco-friendly methods of preparation to preserve the environment. Most of the methods available today are expensive, environmentally harmful, and inefficient with respect to mass production. The present review has explored the Rheological Phase Reaction (RPR) method, which has been extensively utilized as an eco-friendly industrial method for the preparation of metal oxides and metal oxide/carbon composite for lithium ion battery applications. Based on the literature reports, this review has two motivations: to identify the Rheological Phase Reaction (RPR) as the mass production method for preparing metal oxides, metal oxide/carbon composites, and other materials for different applications, to discuss the preparation steps involved, its advantages, the drawbacks associated; and to give a detailed review of the electrochemical performance of different metal oxides by the RPR method for application on the lithium ion battery, with particular emphasis on lithium trivanadate (LiV₃O₈).

Keywords: rheological phase reaction; metal oxides; battery; LiV₃O₈



Citation: Pavithra, S.; Sakunthala, A.; Reddy, M.V.V. Rheological Phase Reaction (RPR) as an Industrial Method for the Production of High Quality Metal Oxides towards Battery Applications. *Energies* **2023**, *16*, 841. <https://doi.org/10.3390/en16020841>

Academic Editor: Carlos Miguel Costa

Received: 20 December 2022

Revised: 5 January 2023

Accepted: 6 January 2023

Published: 11 January 2023



Copyright: © 2023 by the authors. Licensee MDPI, Basel, Switzerland. This article is an open access article distributed under the terms and conditions of the Creative Commons Attribution (CC BY) license (<https://creativecommons.org/licenses/by/4.0/>).

1. Introduction

Metal oxides are an extremely important class of materials from both scientific and technological viewpoints. Hence the different approaches to making metal oxides both in bulk and nano size have become a vital area of research. Several methods, such as sol-gel, hydrothermal, reflux method, ball milling, etc., have been utilized for the preparation of metal oxides [1–4]. But each method has serious limitations, for example, not being suitable for mass production, expensive, time consuming, composed of toxic materials, and others. Apart from these limitations, the major concern about all the above methods of preparation is the environmental pollution they cause. Environment pollution happens when the contaminated solvents utilized in the metal oxide preparation experiments are exposed to their surroundings. Whereas metal oxides are utilized for the removal of heavy metal ions [5], dye degradation [6], energy storage devices [7], solar cells [8], and other applications, the method of preparing metal oxides by themselves should not harm the environment.

On the other hand, research activities on metal oxide preparations cannot be stopped as they are the major steps in achieving high efficiency in a particular process such as dye degradation or the production of high-performance devices. The material preparation plays a major role in determining the performance and as well as the cost of the final devices. The preparation method influences the properties of metal oxides such as phase purity, particle size, surface area, and others, where the metal oxides utilized in lithium ion batteries (LIBs) is just one of the examples. LIB has applications for all portable electronic devices such as mobile phones, laptops, etc. But still, improvements in energy density and power

density are always needed owing to customer expectations. There is a growing demand for high-performing LIB for electric vehicles. To increase the performance and efficiency of LIBs utilized in electronically powered devices and electric vehicles [9,10], the cathode materials such as LiCoO_2 , LiMnO_2 , LiCoPO_4 , LiMn_2O_4 , LiNiO_2 , LiFePO_4 , $\text{Li}_2\text{FeSiO}_4$, and $\text{Li}_3\text{V}_2(\text{PO}_4)_3$ have been explored by preparing them through various preparation routes [11–18]. Among the several methods such as solid-state reaction [19], sol-gel [20], hydrothermal [21], rheological phase reaction (RPR) [22], ultrasonic treatment [23], freeze-drying [24], microwave-assisted sol-gel [25], and spray pyrolysis [26], the RPR method was found to be very promising as an eco-friendly mass production method and meets the industrial demands for preparation of metal oxides for high performance LIBs.

Lithium trivanadate LiV_3O_8 (LVO) is the highly explored material prepared by the RPR method, as observed through our review. Since most of the above cathode materials for LIBs have practical capacities lower than 200 mAh/g [10], LiV_3O_8 , proposed by Wadsley in 1957, rapidly developed among them due to its high theoretical capacity of 352.5 mAh/g as a cathode for the lithium ion battery [27,28]. At the same time, LVO exhibits serious limitations such as fast capacity decay, multiple plateau regions during the charge/discharge process, growth of dendrite, irreversible phase transition, and dissolution of LVO grains during cycling [10]. Although the above limitations were successfully overcome by hetero-ions doping, conductive layer coating, and morphology tuning [22,29–36], still the preparation method adopted plays a crucial role. The phase purity and tuning the morphology of the particles by optimizing the calcination temperatures and time have a major impact [37–41].

Although there are plentiful review reports on different types of cathode materials for LIBs [9,39–41], only seldom are there reports on the review of vanadium oxides for LIBs [42], and particularly the RPR's method of reviewing metal oxides is not a focus in any of the reports. The present report has two main focuses: (1) To discuss the preparation process, steps involved, advantages of RPR as an eco-friendly mass production method, findings from the modified RPR method; and (2) to review the utilization of the RPR method for the preparation of metal oxides and their carbon composites for lithium ion batteries. The report emphasizes the electrochemical performance of the bare and modified LiV_3O_8 material by the RPR method, as it is a much-explored material by this method. Hence the present review of the RPR method can help researchers to choose this method for exploring new metal oxides and help them to bring inventive steps in the RPR method for improving the properties of the metal oxide with no harmful substances being exposed to the environment.

2. What Is Meant by the Rheological Phase Reaction (RPR) Method?

The term “rheology” stands for the study of a material's flow behavior under applied deformation forces or stress. Every material has a property known as viscoelasticity, which indicates both the viscous and elastic portions. If the material is more viscous, it is a liquid; if it is more elastic, it is solid. A proper mixture of metal oxides with appropriate water or organic solvent provides a viscoelastic nature, a property similar to honey. This is called the solid-liquid rheological mixture. In this nature, there is close contact with the reactants and any external heat applied will be uniformly distributed among the reactants with no overheating.

The process of preparing compounds from the solid-liquid rheological mixture through chemical reactions is called the Rheological Phase Reaction (RPR) method. Initially, the stoichiometric molar ratios of the solid reactants (raw materials) are mixed thoroughly using mortar and pestle. Later, the solid-liquid rheological mixture is obtained by adding an appropriate amount of water or other organic solvents (one or two drops) to the well mixed solid reactants, in which the solid particles and liquid substance are uniformly distributed. The resultant mixture will be smooth and viscoelastic as the honey (Figure 1a–c). Finally, the obtained rheological body is transferred to the high pressure reactor and kept at a constant temperature and pressure for an appropriate time. The rheological body collected

from the high pressure reactor is then dried in a petri dish for the desired time until the dry powders are obtained. The smooth powders are then calcinated at the desired temperature and time to obtain the required compounds. The schematic illustration of rheological phase reaction method is shown in Figure 1d.

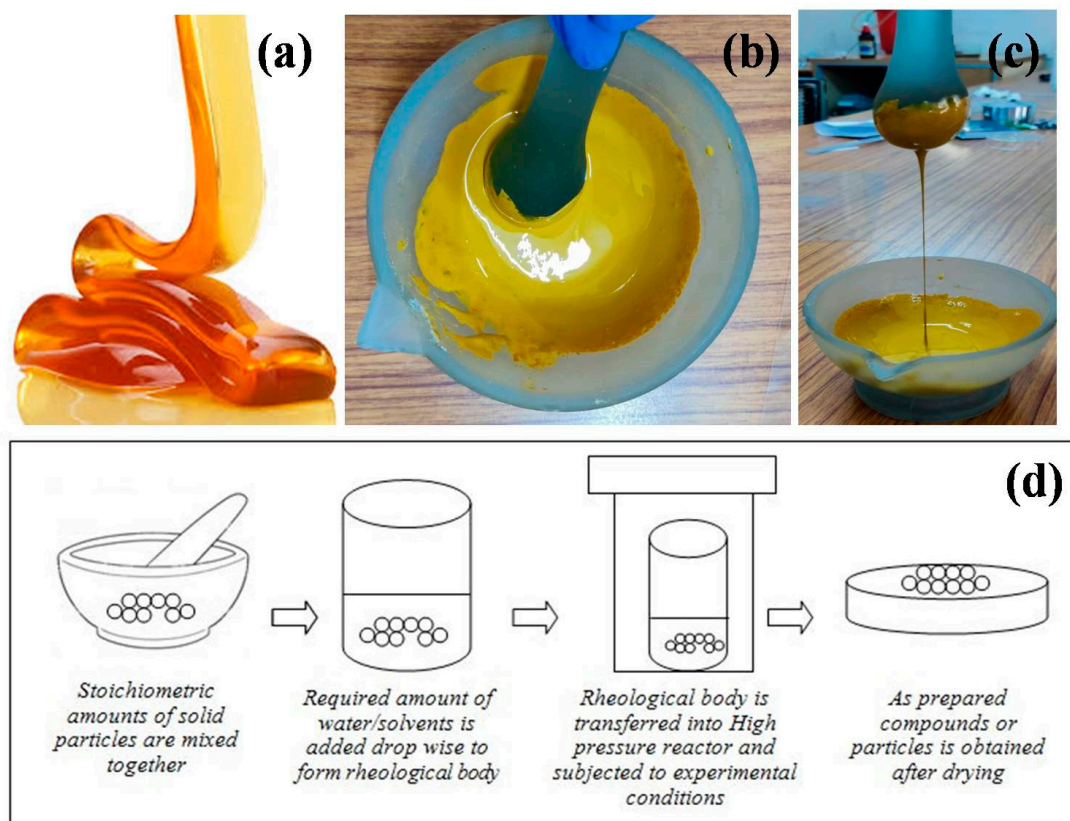


Figure 1. (a) Viscoelastic honey (b,c) a rheological mixture from the laboratory; (d) Schematic illustration of rheological phase reaction method.

Although both the water and organic solvents could be used as the rheological liquid, when water is used as the solvent, there is a great chance that the product may be agglomerated; as the use of an organic solvent is supposed to decrease the particle size. Still, the researchers prefer water as the solvent due to its eco-friendly nature and can overcome the agglomerations through inventive steps. Hence, the RPR method could be classified as the aqueous RPR and non-aqueous RPR method based on the solvent chosen.

3. Advantages of Rheological Phase Reaction as a Pollution-Less Method

Usually, methods such as coprecipitation, sol-gel, hydrothermal, etc., when using high amounts of water or organic solvents are regarded as the best methods for making nanomaterials for mass production. However, all these preparation routes utilize a high volume of water or organic solvents. As a result, the waste water or solvents containing transition metal ions, and other groups such as sulphides, chlorine, fluorine, etc. are harmful to the land and aquatic bodies. In this perspective, the RPR method is considered a “pollution-less method” to prepare any metal oxides with high crystallinity, phase purity, and fewer agglomerations depending on the proper raw materials and the right temperature conditions are being chosen. As discussed before, the preparation steps in RPR involve one or two drops of water/solvent to make the rheological mixture.

Shi X et al. [43] reported on the industrially important zinc borate ($2\text{ZnO}\cdot 3\text{B}_2\text{O}_3\cdot 3\text{H}_2\text{O}$) by the RPR method using zinc oxide (ZnO) and boric acid as the raw materials. The authors reported the RPR method as the “Green Route” with no pollution, and reported the method

as giving a yield of 100% of the theoretical value. The authors have emphasized that the complete conversion of the starting materials can be achieved only in the presence of 0.04 mL water (one drop). The authors reported that the zinc borate formation was closely affected by the water volume, sealing state, reaction time, and temperature.

The lithium nickel cobalt manganese oxide ($\text{LiNi}_{0.6}\text{Co}_{0.2}\text{Mn}_{0.2}\text{O}_2$) is used in LIB applications as a potential cathode material [44]. It has a rich nickel ion content, providing high capacity and a low content of cobalt and manganese ions, stabilizing the structure during the lithium ion intercalation/deintercalation process. The Coprecipitation method is considered the best method for the preparation of the above material for delivering high performance, as it offers control towards morphology control [45–49]. But the coprecipitation method and similar methods involve complex steps such as filtration, purification, and drying of the $\text{Ni}_{0.6}\text{Co}_{0.2}\text{Mn}_{0.2}(\text{OH})_2$ precursor before it can be mixed with the lithium source. Importantly, coprecipitation and similar methods produce large amounts of waste water with metal ions such as sulphate, and other transition metal ions disposed to the environment. Based on the above drawbacks, Xie T et al. [50] introduced the RPR method for the preparation of $\text{LiNi}_{0.6}\text{Co}_{0.2}\text{Mn}_{0.2}\text{O}_2$ and reported the RPR method to be a green and facile method. The authors reported RPR to be a most appropriate method for making $\text{LiNi}_{0.6}\text{Co}_{0.2}\text{Mn}_{0.2}\text{O}_2$ in a well crystalline form, which is crucial for electrochemical performance. The authors emphasized that the RPR method had no complex procedures or environmental issues as in the case of the coprecipitation method.

In the above report, the author mixed stoichiometric amounts of transition metal ion sources NiO, Co_3O_4 , and MnO_2 with the lithium hydroxide monohydrate, ($\text{LiOH}\cdot\text{H}_2\text{O}$) source. Citric acid was added, and all these materials were ground well by ball milling using only 5 mL of distilled water. This formed a rheological phase. The rheological body was dried for just 2 h to obtain the precursor. Later, the precursor was calcinated at 500 °C for 8 h and later at 900 °C for 10 h in the air to yield carbon-coated $\text{LiNi}_{0.6}\text{Co}_{0.2}\text{Mn}_{0.2}\text{O}_2$. The material prepared using citric acid was found to have a well-ordered structure, with very low cation disorders which are usually reported in the case of the above materials by different routes [50]. The highest discharge capacity of 177 mAh/g was recorded for the potential window of 2.5 to 4.3 V.

4. Modified RPR Methods

It is observed from the literature that the RPR method can be modified by different approaches to improve the properties of the prepared materials as below.

4.1. Modified RPR by Ball Milling

Wang W et al. [51] in 2018 introduced the two-step ball milling approach for the preparation of Metallic Cobalt Modified MnO-C nanocrystalline as an efficient bifunctional oxygen electrocatalyst. The rheological phase mixture was obtained by ball milling cobalt acetate and manganese acetate with citric acid and the required amount of water as the solvent. During this process, the cobalt (II) and manganese (II) ions react with citric acid to form the chelate complex. After pyrolysis, the cobalt salt will be reduced to metallic cobalt, and manganous salt will be decomposed into manganese monoxide, and the citric acid will be carbonized into carbon matrices. The precursor was analyzed using a scanning electron microscope (SEM), and it was discovered to have irregular block morphology, indicating that there had been substantial and widespread chelation between metal ions and citric acid throughout the rheological phase reaction process. The irregular blocks were powdered into irregular granules after calcination, and they had good dispersion and uniform nanometric size. The material by this ball milling added to the RPR method gave comparable electro catalytic properties and superior methanol tolerance relative to commercial platinum black catalyst towards Oxygen Reduction Reaction (ORR). In the above report, it is concluded that the ball milling might have acted as a deforming force in tuning the viscoelastic nature of the rheological mixture. The authors noticed widespread

chelation that occurred between metal ions and citric acid during the rheological phase reaction process.

Similar to the above report, the ball-milling step was incorporated for battery material as below. Liu H et al. [52] reported on the design and the synthesis of $\alpha\text{-Fe}_2\text{O}_3\text{@Fe}_3\text{O}_4$ heterostructured anode materials for LIB using the ball-milling assisted RPR method followed by carbothermal reduction. The authors utilized alcohol as the solvent. The iron sources were mixed with citric acid, to which alcohol was added in the presence of ultrasound. The mixture was then ball milled for 1 h and evaporated at 80 °C to remove excess alcohol. The dry powder was calcinated at different temperatures 250–500 °C for 2 h in an argon atmosphere to undergo carbothermal reduction. This resulted in carbon-coated $\alpha\text{-Fe}_2\text{O}_3\text{@Fe}_3\text{O}_4$ heterostructures. The authors have not mentioned the volume of alcohol or the type of alcohol used in the above process. But the authors have emphasized that it is because of the ball milling combined RPR process, the carbonization of citric acid occurred at a low temperature of just 250 °C. With a further increase in calcination to 400 and 500 °C, the outstanding graphitization of amorphous carbon was reported through the Raman spectrum. The authors analyzed the pyrolysis process of citric acid through thermogravimetric analysis (TGA) and Fourier transform infrared spectroscopy (FTIR) characterizations, which revealed the type of reducing gases that were produced. The citric acid used in the RPR method was found to produce CO and CH₄ as the reducing gas, which reduced the iron source. The heterostructures were reported to have a reversible capacity of 711 mAh/g for 0.5 A/g.

4.2. Modified RPR by Three-Step Approach

With the success of the utilization of the RPR method for the LiV₃O₈ materials (to be discussed later), Cao X et al. [53] in 2018 reported on the NaV₃O₈ (NVO) by RPR method with superior rate capability and cycle stability as cathode materials for sodium-ion batteries. The authors prepared NVO by ball milling NaNO₃, NH₄VO₃, and C₆H₈O₇·6H₂O reactants followed by mechanical stirring in a few drops of distilled water until a liquid rheological state appeared. Later, the mixture was autoclaved at 80 °C for 10 h, then the powders calcinated at 300–450 °C for 10 h. The authors implemented three different steps of ball milling (to increase the surface area of reactants), mechanical stirring (to form a rheological mixture), and autoclave (to kindle the chemical reactions). A variation in morphology was observed with the variation in the calcination temperature. The sample calcinated at 350 °C showed a more uniform, smoother, and nanorod-like morphology. The electrochemical performance indicated that NaV₃O₈ could be an alternative cathode material for high performance sodium-ion batteries. With remarkable cyclic performance, a specific discharge capacity of 120 mAh/g was attained at the current density of 120 mA/g and showed an excellent rate capability of 80.8 mAh/g at the current density of 300 mA/g.

4.3. Modified PRP Method Using Liquid Raw Material Source

Yin SY et al. [54] reported the preparation of spinel Li₄Ti₅O₁₂ (LTO) material as a modified RPR method by the utilization of tetra-n-butyl titanate liquid as the source of titanium, where usually a solid source is utilized in the case of conventional RPR methods. The authors mentioned that this kind of approach need not have additional steps such as ball milling, two-step calcination processes, and other processes for the production of phase-pure material. The authors took lithium acetate and tetra-n-butyl titanate liquid as the lithium and titanium raw materials, respectively. The raw materials were ground well using mortar and pestle for more than half an hour. Later a trace of water was added to accelerate the hydrolysis of tetra-n-butyl titanate, and ground well for a few minutes, which produced a rheological body for further calcination process. The authors also compared the phase purity of the materials with and without autoclaving the rheological body before the calcination step. The authors proved the role of the heat treatment step through the X-ray diffraction (XRD) pattern of the precursors with and without autoclaving before the calcination process (as shown in Figure 2).

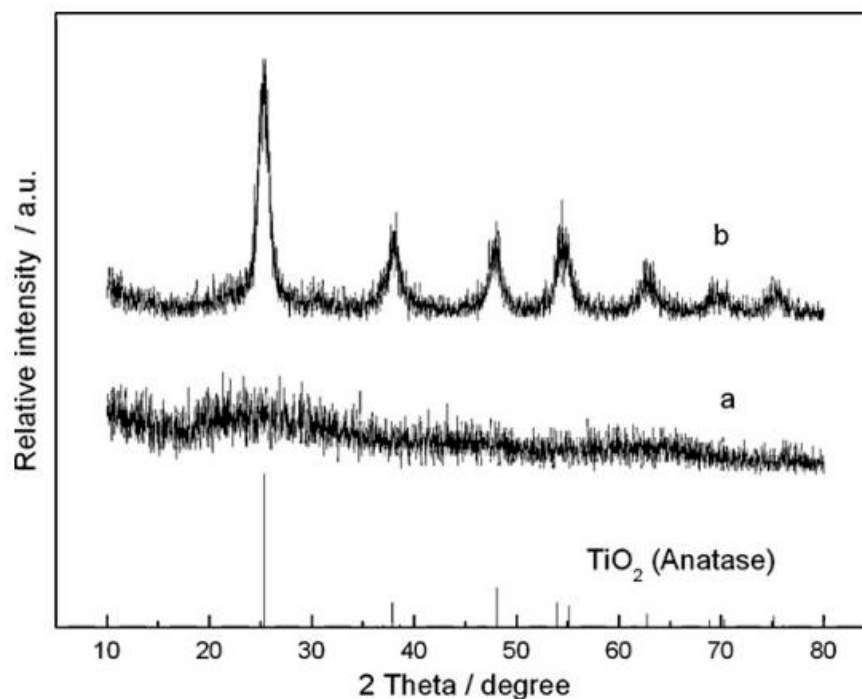


Figure 2. XRD pattern of the precursors with heat treatment (autoclaved) (represented as 'a' in the graph) and without heat treatment (represented as 'b' in the graph). Reprint with permission [54]; Copyright © 2009 Elsevier Ltd. All rights reserved.

The precursor with heat treatment before the calcination process was found to be the TiO₂ anatase phase. Changes in morphology were also observed using SEM analysis. Precursors that had had heat treatment revealed individual particles with smaller average particle sizes and narrower particle size distributions, whereas precursors that had undergone no heat treatment displayed a disordered morphology made up of agglomerated particles. The LTO prepared from calcination of heat treated precursor in the RPR method at 800 °C for 12 h was found to deliver 180 mAh/g of discharge capacity for 1 C current rate in the potential window of 1–3 V, which was only 160 mAh/g in case of LTO made with precursor without heat treatment for a similar calcination temperature. The authors also emphasized the role of calcination temperature on the structural property of LTO and optimized the material for a calcination temperature of 800 °C for 12 h. The authors mentioned that the RPR method is the only suitable method for the preparation of LTO material with a narrow size distribution, which is not possible in the case of solid-state methods.

4.4. Coprecipitation Assisted RPR Method

Shi X et al. [55] reported on the spherical Li_{1+x}Ni_{0.5}Mn_{0.5}O_{2+δ} by preparing the raw materials for RPR by the coprecipitation method. The spherical Ni_{0.5}Mn_{0.5}CO₃ carbonate precursor was initially prepared by the coprecipitation route (Figure 3).

LiOH was added and a rheological body was obtained using distilled water by a stirring process, autoclaved at 80 °C for 4 h. The mixture was obtained with no grinding process such that the spherical morphology of the raw material prepared by the coprecipitation route was not disturbed. The mixture was sintered at 600 °C for 5 h before calcination at 900 °C for 16 h. It is found that this modified RPR method with no grinding process was successful in forming phase-pure intended material with destruction in the shape of the precursor used. The prepared material Li_{1+x}Ni_{0.5}Mn_{0.5}O_{2+δ} retained the shape of the carbonate precursor Ni_{0.5}Mn_{0.5}CO₃ (Figure 4). It was possible to attain a high discharge capacity of 200 mAh/g and outstanding cycling performance with zero capacity decay after 100 cycles at 20 mA/g. But the disadvantage associated with this approach is the pollution of the environment as discussed before.

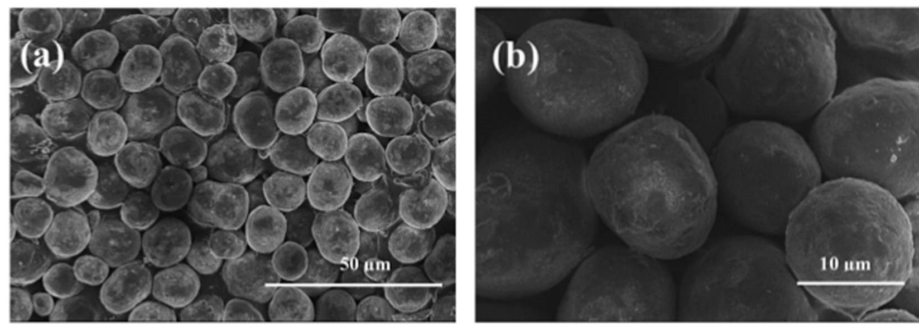


Figure 3. SEM images of spherical $\text{Ni}_{0.5}\text{Mn}_{0.5}\text{CO}_3$ carbonate by the Coprecipitation route at (a) 50 μm and (b) 10 μm . Reprint with permission [55]; © 2014 Elsevier Ltd. All rights reserved.

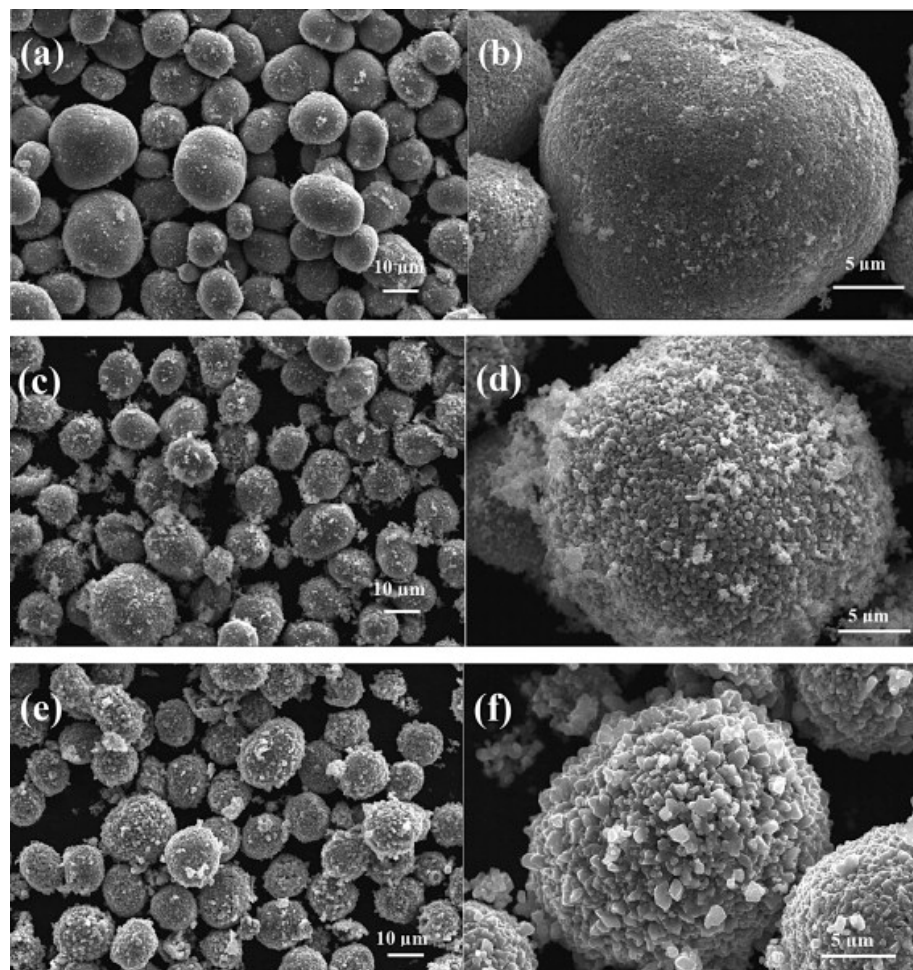


Figure 4. SEM images of spherical $\text{Li}_{1+x}\text{Ni}_{0.5}\text{Mn}_{0.5}\text{O}_{2+\delta}$ made from spherical $\text{Ni}_{0.5}\text{Mn}_{0.5}\text{CO}_3$ carbonate precursor by Coprecipitation assisted RPR method (a,b) $x = 0$, (c,d) $x = 0.1$ and (e,f) $x = 0.2$ Reprint with permission [55] © 2008 Elsevier Inc. All rights reserved.

4.5. RPR Assisted Microwave Method

Yan J et al. [56] reported for the first time on the $\text{Li}_3\text{V}_2(\text{PO}_4)_3/\text{C}$ cathode by RPR-assisted microwave method. The rheological mixture was made using the stoichiometric amount of raw materials, Li_2CO_3 , $\text{NH}_4\text{H}_2\text{PO}_4$, and V_2O_5 were mixed with citric acid and 1.5 mL of PEG and the appropriate amount of distilled water to get the rheological body. Both poly(ethylene glycol) (PEG) and citric acid were used as the carbon source. PEG also served as the rheological medium. This rheological mixture was initially sintered at 350 °C for 4 h and subjected to microwave irradiation for just 15 min. This method resulted

in uniformly carbon-coated $\text{Li}_3\text{V}_2(\text{PO}_4)_3$ pristine particles by calcination under an inert atmosphere. This method benefitted from the merits of both the preparation routes, where the $\text{Li}_3\text{V}_2(\text{PO}_4)_3/\text{C}$ composite was reported to deliver an ultrahigh specific capacity of 101.8 mAh/g at 50 C rate with the significant cycling life. The role of microwave heating in the above process was to reduce the calcination temperature.

Very recently, a similar approach to microwave assisted RPR method was reported by Liu H et al. [57] for the preparation of $\text{Cu}_3\text{Mo}_2\text{O}_9$. The authors reported the material to have both the lithium storage capability for lithium-ion battery applications and as a supercapacitor as well. As an anode for LIB, the material delivered 554.6 mAh/g after 350 cycles, and as a super-capacitive material, it delivered 136.3 F/g after 1000 cycles. The authors strongly suggested that their work has opened a new avenue to prepare efficient inorganic materials through the RPR method.

5. Role of Preparation Temperature and Holding Time in the RPR Method

The preparation temperature and the holding time for the preparation of materials have to be optimized in the case of the RPR method, as suggested in many reports. The reports on iron borate compounds such as Fe_3BO_6 show that it is very difficult to prepare them in phase-pure nature, which requires calcination at very high temperatures or repeated heat treatments. This is due to the slow diffusion of ions in the solid state medium. Shi X et al. [58] reported on the Fe_3BO_6 phase-pure nano spherical particles by the RPR method. The as-prepared materials were found to be spherical nano crystals. The authors reported the RPR method to be a simple, economical, and efficient soft chemistry method for the making of iron borates. The authors prepared the material using H_3BO_3 and $\text{FeC}_2\text{O}_4 \cdot 2\text{H}_2\text{O}$, where the raw materials were uniformly mixed using a little drop of water. The authors emphasized that the RPR method avoids local heating and aided the efficient heat exchange. The authors have proposed (i) dehydration and (ii) decomposition as the two major steps involved in the RPR method. In the above approach, based on the thermal analysis of the precursor and the XRD studies at different temperatures, the reaction was proposed as below,

The dehydration of H_3BO_3 and decomposition of $\text{FeC}_2\text{O}_4 \cdot 2\text{H}_2\text{O}$:

FeO obtained from the decomposition of $\text{FeC}_2\text{O}_4 \cdot 2\text{H}_2\text{O}$ is then oxidized to Fe_3O_4 and finally to Fe_2O_3 .



Later the B_2O_3 melts and reacts with the above product by getting coated over Fe_2O_3 to form the Fe_3BO_6 phase-pure nano spherical particles. The RPR approach has avoided troublesome processes such as quenching, regrinding, and repeated sintering and calcination. The calcination time was only 5 h and 3 h at a temperature of 800 and 900 °C, respectively. Otherwise, it would have been 48 h at 880 °C, in the case of the solid state method for the same material.

Fe_3BO_6 prepared at 800 °C for 5 h was formed as well spherical particles (Figure 5a) of uniform size of about 40 nm. Just the increase in calcination temperature to 900 °C resulted in uniform nano spherical particles of increased diameter of 100 to 500 nm (Figure 5b). The grains agglomerated randomly by an increase in calcination temperature. The particles prepared at 800 °C for 5 h were found to act as the best anode material with a high reversible capacity of about 500 mAh/g with a significant depth of discharge.

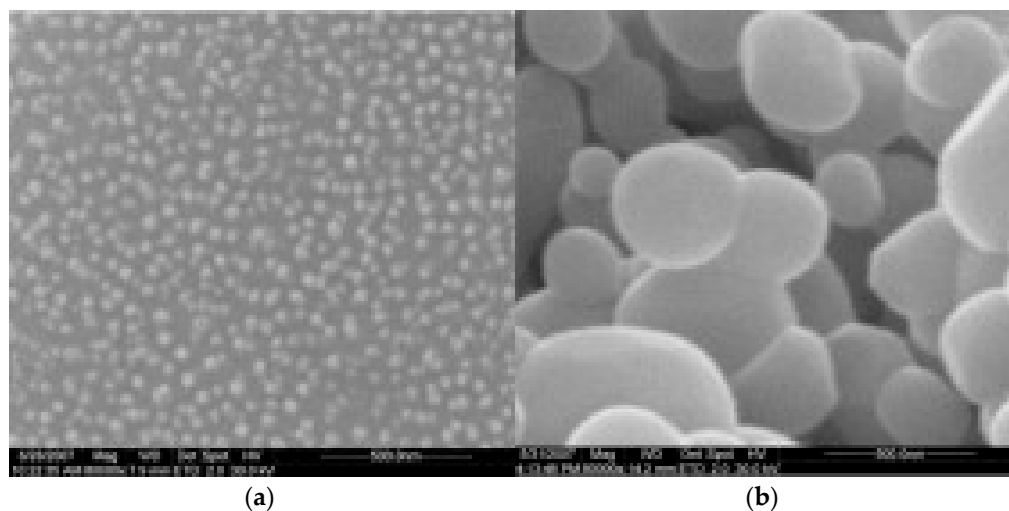


Figure 5. SEM images of Fe_3BO_6 powders calcinated at (a) $800\text{ }^\circ\text{C}$ for 5 h and (b) $900\text{ }^\circ\text{C}$ for 3 h. Reprint with permission [58] © 2008 Elsevier Inc. All rights reserved.

Peng H et al. [59] reported on the role of preparation temperature and holding time for $\text{LiNi}_{1/3}\text{Co}_{1/3}\text{Mn}_{1/3}\text{O}_2$ cathode material using the RPR method. The authors reported the high calcination temperature of $900\text{ }^\circ\text{C}$ for 8 h to be more suitable for the formation of a highly ordered layered structure with low cation mixing. This material delivered a maximum discharge capacity of 198 mAh/g at 0.2 C rate between 2.5 to 4.6 V.

Huang X et al. [60] prepared Li_2MoO_4 as an anode material for lithium storage and found the key calcination temperature to be $700\text{ }^\circ\text{C}$. Even at such high calcination temperatures, the material was found to have particles of size 100 to 300 nm. The authors found this method to be more suitable for making the above material in phase-pure form with lower particle size. The material showed a good electrochemical performance of 592 mAh/g at 0.2 mA/cm^2 current density and was found to possess $\sim 75\%$ of capacity retention even after 50 cycles.

As discussed above, the RPR method can be combined with any other methods for the successful preparation of materials. New inventive steps are yet to be explored in the case of the RPR method, as this method is found to be suitable for making industrial products with no harm to the environment. For example, Zheng H et al. [61] reported on the nanorod morphology of $\text{KMn}_8\text{O}_{16}$, even in the absence of citric acid or any other, just with one drop of water for making a rheological mixture. The above material calcinated at $300\text{--}500\text{ }^\circ\text{C}$ was found to be nanorods in the range of 5–20 nm and length around 100–300 nm (Figure 6). The material prepared at $400\text{ }^\circ\text{C}$ was found to exhibit the best electrochemical performance as a cathode material for lithium insertion, with a discharge capacity of 147.9 mAh/g even after 80 cycles at the current density of 50 mA/g . This approach indicates that the RPR method is a simple, cost-effective, and efficient method for making nanomaterials.

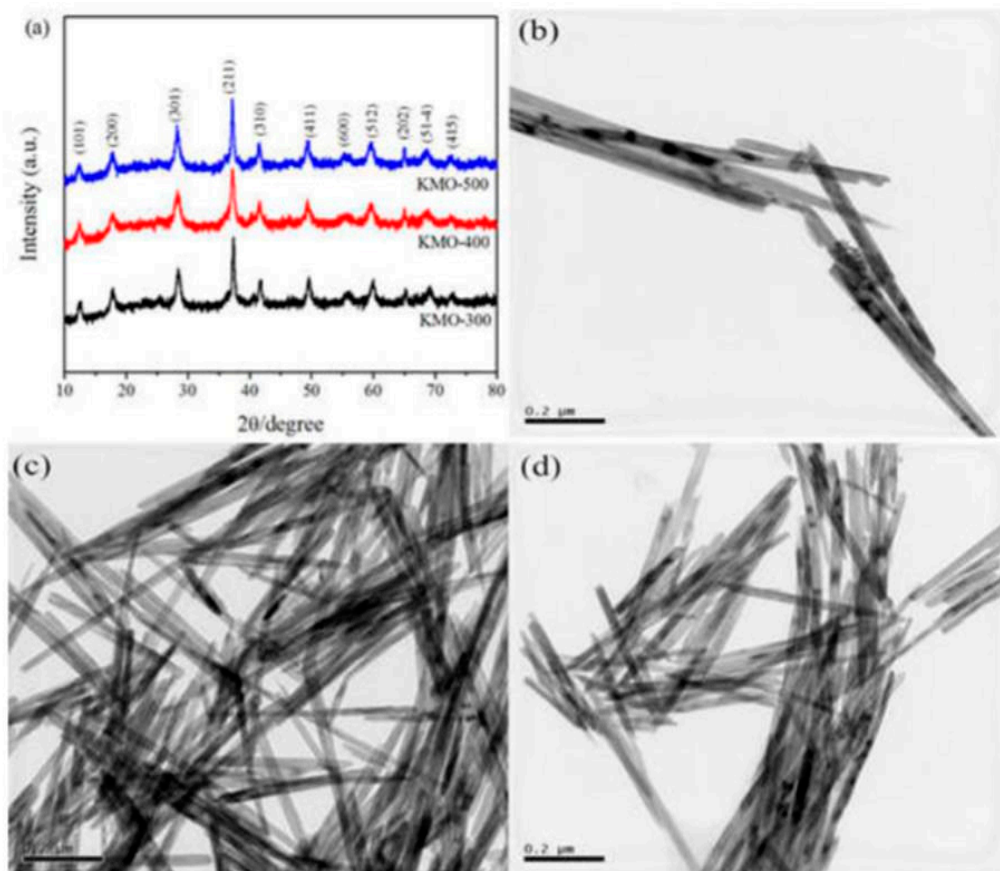


Figure 6. (a) XRD patterns of $\text{KMn}_8\text{O}_{16}$ and SEM images of $\text{KMn}_8\text{O}_{16}$ prepared at (b) 300 °C, (c) 400 °C and (d) 500 °C Reprint with permission [61] © IOP Publishing Ltd.

6. Carbon-Coated Materials by RPR Method

The RPR method was found to be more suitable for the making of carbon-coated materials for different applications, and more particularly for energy applications. Carbon acts as the electronic path in the electrode and aids in better results. Li Y et al. [62] reported on the preparation of carbon-coated $\text{LiMn}_{0.8}\text{Fe}_{0.2}\text{PO}_4$ materials via the RPR method using three different carbon sources such as citric acid, glucose, and sucrose. The carbon coating was found to enhance the electrochemical performance of the above material both in capacity and in cycle stability. The above material was made by mixing a stoichiometric ratio of metal ion sources in deionized water to make a viscous slurry, to which citric acid/glucose/sucrose was added and stirred at 70 °C and ball milled for 7 h to form a rheological body. Although in many reports, the residual water was removed by a drying process in a petri dish or pressurized autoclave for a few hours, here the authors removed the residual water by freeze drying. In either case, there is no harm to the environment. Later, the precursor was calcinated at 650 °C for about 8 h under a nitrogen atmosphere to form carbon-coated $\text{LiMn}_{0.8}\text{Fe}_{0.2}\text{PO}_4$. The authors mentioned that the type of carbon source chosen has an important effect on the formation of the rheological phase as well as on the composition and structure of the surface carbon layer coated. When the citric acid was used as the rheological medium or as carbon sources, the particles were found to have homogenous distribution in size with a Brunauer-Emmett-Teller (BET) specific surface area of 50 m^2/g , than by using glucose or sucrose with a BET surface area of 40 and 22 m^2/g respectively. The material made using citric acid was reported to have mesoporous nature, which is essential for efficient battery performance. The authors proved the presence of carbon through XPS analysis with a peak at 284.7, 286.3, and 288.7 eV, which can be regarded as the sp^2 carbon of C–C bonds, C–N bonds, and N–C=N bonds, respectively, beneficial for the ion diffusion kinetics. The above peak was found to be intense in case of the

carbon coating using citric acid as the carbon source. Based on the electrochemical results, the authors reported that citric acid acted as the best carbon source for making carbon-coated $\text{LiMn}_{0.8}\text{Fe}_{0.2}\text{PO}_4$ materials via the RPR method. The carbon-coated $\text{LiMn}_{0.8}\text{Fe}_{0.2}\text{PO}_4$ delivered a discharge capacity of 164 mAh/g at 0.1 C and 99.6% of capacity retention after 100 cycles at 1 C rate.

Wu Y et al. [63] have prepared carbon-coated $\text{Li}_3\text{V}_2(\text{PO}_4)_3$ by a modified RPR method using alginic acid as the new carbon source and found the material to possess a three-dimensional carbon network with impressive electrochemical performance between 3 to 4 V at 0.5 C rate. The material by alginic acid-assisted RPR method achieved significant capacity close to its theoretical capacity and was reported to deliver a high capacity even at 40 C current rate, thanks to the RPR method, where the materials are proven to be industry-ready materials. This shows the RPR method to be the best method for making carbon composites or carbon-coated materials with a good 3D network in a green way.

Zhong YJ et al. [64] reported on the carbon-coated lithium manganese iron phosphate solid-solution materials by RPR method utilizing stearic acid as the carbon source. The authors utilized ethanol as the dispersing medium instead of water. Lithium carbonate (Li_2CO_3), manganese carbonate (MnCO_3), ammonium dihydrogen phosphate ($\text{NH}_4\text{H}_2\text{PO}_4$), and iron (III) phosphate tetrahydrate ($\text{FePO}_4 \cdot 4\text{H}_2\text{O}$) were used as the raw materials and the mixtures were ball milled with ethanol to obtain the rheological body. Finally, the resulting precursor was thermally treated in a tube furnace at 350 °C for 2 h, then at 600 °C for 5 h under an inert atmosphere to yield the carbon composite materials $\text{LiMn}_{0.5}\text{Fe}_{0.5}\text{PO}_4/\text{C}$, $\text{LiMn}_{0.2}\text{Fe}_{0.8}\text{PO}_4/\text{C}$, and $\text{LiMn}_{0.8}\text{Fe}_{0.5}\text{PO}_4/\text{C}$. The materials were found to be coated with a few layers of carbon. Here stearic acid was found to play both the role of a surfactant to uniformly mix the raw materials, to reduce the size of the particles, and also as a carbon source. The materials were reported to exhibit excellent electrochemical performances.

Hu Y et al. [65] has reported on the α - LiFeO_2 material by the RPR method with a higher crystalline degree and nanosized particles for lithium ion battery applications. The particle sizes ranged from 100 to 300 nm. The material delivered a discharge capacity of 169 mAh/g at 0.1 C between 1.5 and 4.3 V. The higher crystalline degree of the above material by the RPR method was found to be the reason for the good performance of the α - LiFeO_2 material.

7. Critical Review on the Preparation of LiV_3O_8 by RPR Method

The LiV_3O_8 is found to be the most explored electrode material for LIB, as it is supposed to have a high theoretical capacity as a cathode. The LIB made with this material is considered to deliver higher energy density. The only drawback associated with this material is that the lithium ions in LiV_3O_8 act as a pillar and do not take part in the charge-discharge process. Hence, this cathode material has to be combined only against lithium metal for the LIB application, where the material is to be first discharged to act as a cathode. However, few reports have demonstrated the chemically lithiated LiV_3O_8 , where the material can be used in LIB against any anode and hence can be charged initially. Apart from this drawback, the material is still being explored as a cathode material owing to its high capacity by the multivalent oxidation states of vanadium. The RPR method has been extensively utilized for the preparation of LiV_3O_8 by various authors, and the results are presented below.

7.1. RPR as a Low Temperature Route for LiV_3O_8

To prepare bare LiV_3O_8 , most of the authors used lithium hydroxide monohydrate ($\text{LiOH} \cdot \text{H}_2\text{O}$) as the lithium source [10,22,36,38,66–71] and only a few authors utilized lithium acetate ($\text{CH}_3\text{COOH} \cdot 2\text{H}_2\text{O}$) as the lithium source [36]. In a majority of cases, ammonium metavanadate (NH_4VO_3) [10,36,37,67–71] was utilized as the vanadium source, and a few report on vanadium (V) oxide (V_2O_5) as the source for vanadium [22,36]. The ascorbic acid ($\text{C}_6\text{H}_8\text{O}_6$) [10], carbamide ($\text{CH}_4\text{N}_2\text{O}$) [38] and citric acid ($\text{C}_6\text{H}_8\text{O}_7$) were mostly utilized as the complexing agents [22,36,37,68–70]. The proper composition of the different lithium

and vanadium sources used to prepare bare and modified LiV_3O_8 by the above reports is shown in Table 1, for the benefit of readers. In all cases, the raw materials are ground well, using mortar and pestle with a few drops of distilled water (one or two drops) to obtain a rheological phase medium. The as-prepared rheological body was then dried at 80–120 °C for 5–12 h either in a petri dish or in a pressurized autoclave. Finally, the dried mixtures were calcinated at a low temperature varying from 300–600 °C for about 10–12 h.

In the case of doped/modified LiV_3O_8 , the corresponding raw materials for the dopants were just added to the lithium and vanadium sources. For example, in the case of erbium (Er)doped material, the $\text{LiOH}\cdot\text{H}_2\text{O}$, NH_4VO_3 , and Er_2O_3 in molar ratio 1:3:0.01 were taken in an agate mortar and grained well. A required amount of distilled water was added to the mixture to obtain the rheological phase. This was subjected to desired heating and drying conditions and was calcinated at 350 °C for 10 h [67]. Here, the authors have demonstrated the formation of Er-doped LiV_3O_8 at a very low calcination temperature, which can be considered an advantage of the RPR method.

Liu Q et al. [36] made a two-step analysis of the precursor: one was from 200 °C to 600 °C and another was after 600 °C. It was seen that the sample weight remained constant at the temperature range of 370–600 °C. In the same way, Sau et al. [35] analyzed the precursor from 60–700 °C and reported that the sample weight was stable above 400 °C. Li W et al. and Zhu L et al. [68,69] reported that no weight loss was found till 1000 °C and 800 °C respectively through single step analysis. From these results, it can be observed that LiV_3O_8 was obtained by burning the precursor from 350–600 °C [37], a process with low calcination temperature.

The main phase of LiV_3O_8 shows a layered monoclinic structure [37,66–68], which belongs to the P21/m space group [37,66–68] and the JCPDS 72-1193 [10,35,37,68–70] was found to be the standard data for bare LiV_3O_8 . The calcination temperature plays a vital role in the LiV_3O_8 phase formation and crystallization. At calcination temperatures of 500–600 °C, the intensities of diffraction peaks were stronger and peak splitting was observed indicating good crystallinity of the material which leads to improved electrochemical performance [36]. At the above temperatures, impurities of V_2O_5 in small amounts were observed and this binary phase (as shown in Figure 7) was reported to have a minor influence on the electrochemical activity of the LiV_3O_8 powder [37,68,70–75]. The presence of broader and low intensity peaks in the diffraction patterns led to poor crystallization, resulting in sluggish kinetics of Li^+ intercalation and de-intercalation processes during discharge/charge cycles and hinders the performances [10,36,70]. When LiV_3O_8 is modified with doping of hetero-atoms, the peak intensities were higher (as shown in Figure 7) and the extended interlayer spacing was observed. This enhances the Li^+ intercalation and de-intercalation processes during discharge/charge cycles [30,33–35,67,68,76–78].

As we observe from Table 1, the morphology of the LiV_3O_8 was found to vary depending on the raw materials chosen. The morphology analysis was carried out using Scanning Electron Microscopy (SEM) and Transmission Electron Microscopy (TEM) analyses. The morphology of LiV_3O_8 highly depends upon the calcination temperature used and it is significant. The particles were larger in size, independent, and well dispersed when synthesized at temperatures >500 °C (as shown in Figure 8) [36,37].

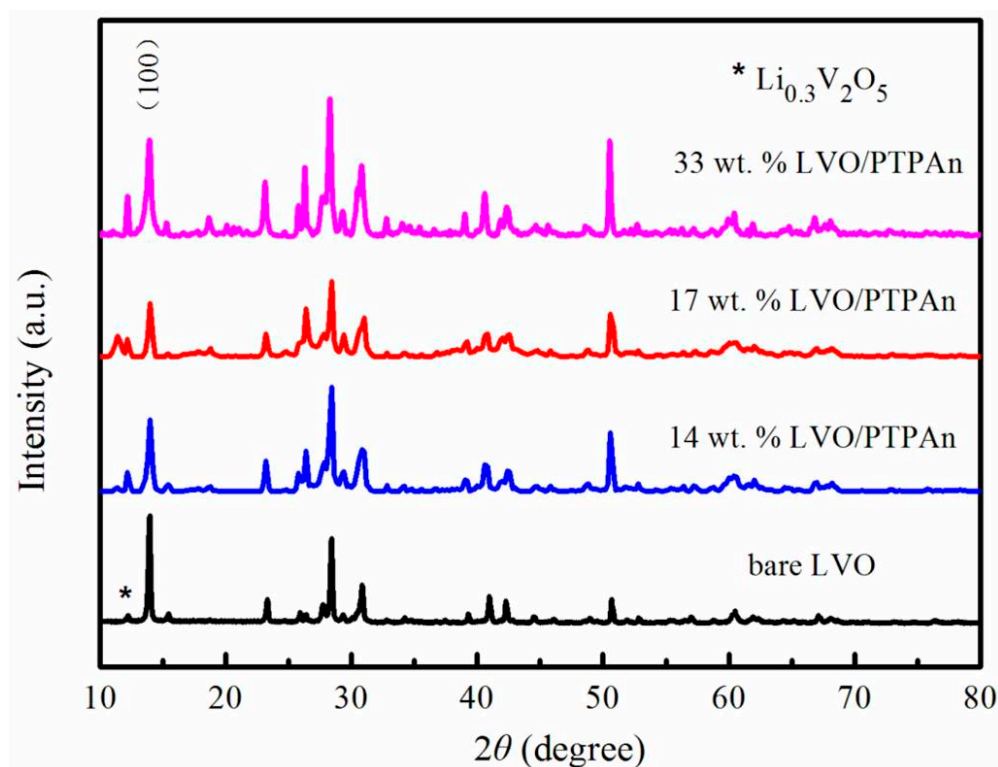


Figure 7. XRD patterns of the bare LiV_3O_8 sample and LiV_3O_8 /Polytriphenylamine (PTPAn) composites Reprint with permission [68] © 2017 by the authors. Licensee MDPI, Basel, Switzerland.

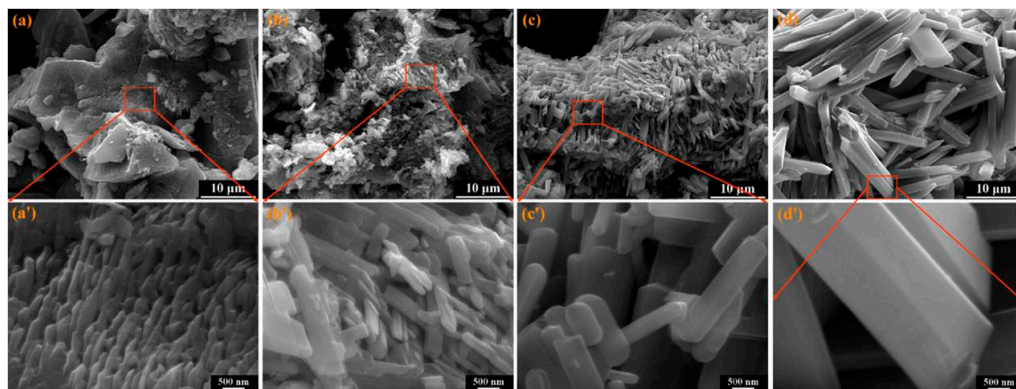


Figure 8. SEM images of LiV_3O_8 powders: (a) 450 °C and (a') magnified image of 450 °C; (b) 500 °C and (b') magnified image of 500 °C; (c) 550 °C and (c') magnified image of 550 °C; (d) 600 °C and (d') magnified image of 600 °C Reprint with permission [37] © 2011 Elsevier B.V. All rights reserved.

On considering modified LiV_3O_8 uniform, small, and evenly distributed particles were obtained when compared to bare LiV_3O_8 , which showed uneven, agglomerated particles restricting the shuttling of Li^+ ions and deteriorating the electrochemical performances [10,66,67].

Table 1. Raw materials used and their corresponding morphology for bare and modified LiV_3O_8 .

Material	Synthesis Method of		Morphology of		Ref.
	Bare LiV_3O_8	Modified LiV_3O_8	Bare LiV_3O_8	Modified LiV_3O_8	
LiV_3O_8	$\text{CH}_3\text{COOLi}\cdot 2\text{H}_2\text{O}$, NH_4VO_3 and citric acid in a molar ratio of 1:3:4	-	Bar-like structures	-	[36]
LiV_3O_8	stoichiometric amounts of $\text{LiOH}\cdot\text{H}_2\text{O}$, NH_4VO_3 and carbamide	-	Rod shaped	-	[37]
Er-Doped LiV_3O_8	$\text{LiOH}\cdot\text{H}_2\text{O}$, NH_4VO_3 in molar ratio 1:3	$\text{LiOH}\cdot\text{H}_2\text{O}$, NH_4VO_3 , Er_2O_3 in molar ratio 1:3:0.01	Uneven distribution with small particles adhering on them	Smaller and more compact particles with uniform distribution	[67]
ZnO-Coated LiV_3O_8	Stoichiometric amounts of $\text{LiOH}\cdot\text{H}_2\text{O}$ and NH_4VO_3	Dispersion of LVO in an ethyl alcohol solution of $\text{Zn}(\text{CH}_3\text{CO}_2)_2\cdot 2\text{H}_2\text{O}$	Crystalline with agglomeration	Strip-like particles with bright ZnO grains	[66]
$\text{Mg}_2(\text{PO}_4)_3$ -coated LiV_3O_8	$\text{LiOH}\cdot\text{H}_2\text{O}$: NH_4VO_3 : $\text{C}_6\text{H}_8\text{O}_7\cdot 6\text{H}_2\text{O}$ in molar ratio 1:3:1	Solution surface deposition of $\text{Mg}(\text{NO}_3)_2$	agglomeration with unevenly distributed grains	Pillar-like structure	[10]
LiV_3O_8 -PPy composite	LiOH , V_2O_5 and citric acid in a molar ratio of 1:1.5:4.8	Simple dispersion of LVO and PPy in ethanol	Needle-like or flake-like structures	Well dispersed	[22]
LiV_3O_8 -PPy composite	$\text{LiOH}\cdot\text{H}_2\text{O}$, V_2O_5 , and citric acid in ratio 1:1.5:4.8	In situ polymerization of the LiV_3O_8 made by the RPR method	Flake-like agglomerates with sharp edges	Well dispersed	[35]
LiV_3O_8 /PTPAn composite	Stoichiometric amounts of $\text{LiOH}\cdot\text{H}_2\text{O}$, NH_4VO_3 , and $\text{C}_6\text{H}_8\text{O}_7\cdot 6\text{H}_2\text{O}$	In situ polymerization of the LiV_3O_8 made by the RPR method	Rough surface Nanorods	Smooth surface nanorods	[68]
LiV_3O_8 /PEDOT composite	Stoichiometric amounts of $\text{LiOH}\cdot\text{H}_2\text{O}$, NH_4VO_3 , and $\text{C}_6\text{H}_8\text{O}_7\cdot 6\text{H}_2\text{O}$	In situ polymerization of the LiV_3O_8 made by the RPR method	Nanorod aggregate	Accumulation of flakiness	[69]
LiV_3O_8 /PDPA composite	Stoichiometric amounts of $\text{LiOH}\cdot\text{H}_2\text{O}$, NH_4VO_3 , and $\text{C}_6\text{H}_8\text{O}_7\cdot 6\text{H}_2\text{O}$	In situ polymerization of the LiV_3O_8 made by the RPR method	Nanorods with slippery surface	Sloppy surface, uniform particles and jagged edges	[70]

7.2. Preparation of Modified LiV_3O_8 by RPR Method with Additional Steps

Cao X et al. [66] prepared LiV_3O_8 by the RPR method and made 1, 2, and 3 wt% of ZnO-coated LiV_3O_8 by dispersing the as-prepared LiV_3O_8 in an ethyl alcohol solution of $\text{Zn}(\text{CH}_3\text{CO}_2)_2\cdot 2\text{H}_2\text{O}$. This was then heated at 80 °C and calcinated at 350 °C for 5 h to obtain ZnO-coated LiV_3O_8 . Xie L et al. [10] prepared (0.5, 1, 1.5, and 2 wt%) $\text{Mg}_2(\text{PO}_4)_3$ -coated LiV_3O_8 by solution surface deposition of $\text{Mg}(\text{NO}_3)_2$, Na_3PO_4 and as-prepared LiV_3O_8 by the RPR method in an ultrasonication process. This solution was subjected to desired heating and drying conditions and the obtained precursor was calcinated at 350 °C for 6 h to get $\text{Mg}_2(\text{PO}_4)_3$ -coated LiV_3O_8 . Both approaches showed a better electrochemical performance with the advantage of low calcination temperature.

7.3. Electrochemical Properties of LiV_3O_8 by RPR Method

It is observed from Table 2 that the doping in LiV_3O_8 material by the RPR method increased the discharge capacity cycling stability of LiV_3O_8 for lithium ion battery applications.

Table 2. Comparison between the electrochemical properties of bare and modified LiV_3O_8 .

Material	Current Density (mAcm^{-2})	Voltage (V)	Initial Capacity of Bare LVO (mAhg^{-1})	Initial Capacity Modified LVO (mAhg^{-1})	Cycles	Final Capacity of Bare LVO (mAhg^{-1})	Final Capacity of Modified LVO (mAhg^{-1})	Ref.
LiV_3O_8	0.3 mAcm^{-2}	1.8–4.0	272.9	-	10	248.5	-	[36]
LiV_3O_8	50	2.0–4.0	273.6	-	60	213.0	-	[37]
Er-Doped LiV_3O_8	30	1.8–4.0	294.2	295.4	50	176.6	220.7	[67]
2 wt% ZnO-Coated LiV_3O_8	30	1.8–4.0	310.67	274.2	20	198.0	240.9	[66]
1 wt% $\text{Mg}_2(\text{PO}_4)_3$ -coated LiV_3O_8	60	1.8–4.0	286.0	323.93	50	169.6	250.82	[10]
LiV_3O_8 -20% PPy composite	40	1.5–3.85	250.0	292.0	40	120.0	250.0	[22]
LiV_3O_8 -PPy composite	40	1.5–3.85	210.0	184.0	100	110.0	183.0	[35]
17% LiV_3O_8 /PTPAn composite	60	1.8–4.0	286.0	275.0	50	169.0	271.0	[68]
20 wt% LiV_3O_8 /PEDOT composite	60	2.0–4.0	264.5	270.0	50	184.5	260.0	[69]
10 wt% LiV_3O_8 /PDPA composite	60	1.8–4.0	286.0	311.0	50	169.0	272.0	[70]

To test the electrochemical performance of the powder samples, different types of coin cells were constructed using lithium metal as an anode, various commercial polymer separators, and electrolytes. To fabricate the cathodes, the slurry was made using different combinations of the prepared LiV_3O_8 as active materials, polyvinylidene fluoride (PVDF) and polytetrafluoroethylene (PTFE) as the binder, acetylene black, ketjen black, which was coated on current collectors. The current density, voltage range, initial charge/discharge capacity of bare and modified LiV_3O_8 , and their corresponding cyclic stability are explained in Table 2. In agreement with the structural and morphology results, doped LiV_3O_8 shows better specific capacity, rate capability, and cyclic retention than bare LiV_3O_8 . As the calcination temperatures play a major role in the electrochemical performance, it is seen that high discharge capacities were obtained for samples prepared at 400–500 °C calcination temperatures using the RPR method [36,37]. The initial charge/discharge capacity was found to be 273.6 mAh/g, which was higher than the traditional synthesis methods [37]. This is mainly because of the high crystallinity, fast electron transport and ion diffusion, and large surface-to-volume ratios of the LiV_3O_8 , which are advantageous for Li^+ intercalation. When suitable wt% of materials are coated on bare LiV_3O_8 , improved specific capacity, cyclic behavior, and capacity retention were observed [10,66]. For example, Xie L et al. [10] reported that coating of 1 wt% of $\text{Mg}_2(\text{PO}_4)_3$ (MP) protective layer on LiV_3O_8 showed an initial charge/discharge capacity of 323.93 mAh/g which was much higher than bare LiV_3O_8 (286.0 mAhg^{-1}), as shown in Figure 9. These coating layers maintained the stability of the LiV_3O_8 crystal structure and were found to inhibit the dissolution of LiV_3O_8 into the electrolyte and exhibited the capacity 250.82 mAh/g even after 50 cycles (as shown in Figure 9). Hence, the RPR method was found to be an excellent method for the preparation of LiV_3O_8 and modified LiV_3O_8 materials for practical applications in energy devices.

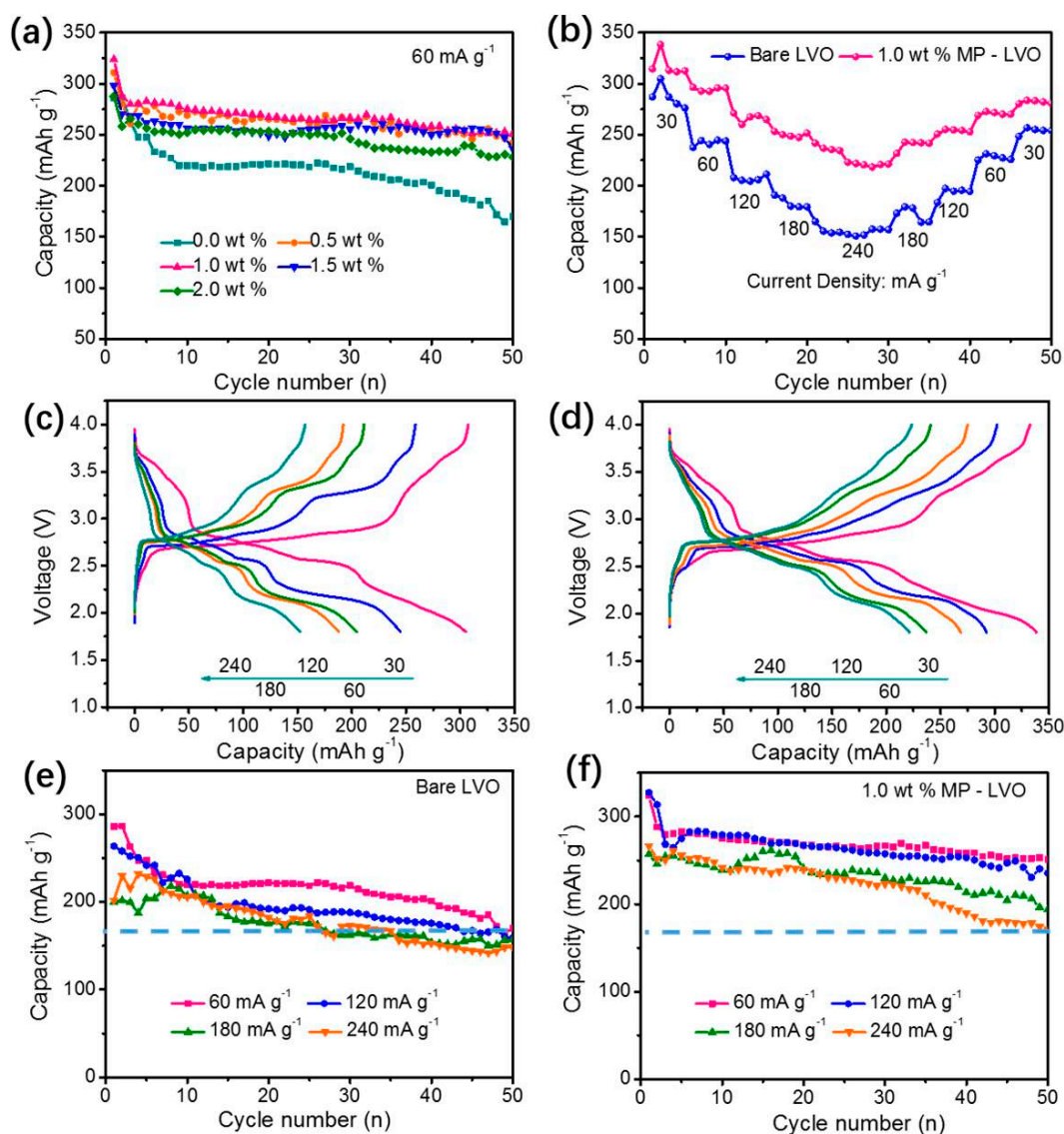


Figure 9. Cycling performance of MP-coated LVO samples with different MP contents at the current rate of 60 mA g⁻¹ with the voltage range of 1.8–4.0 V (a), and stepped rate capabilities of the bare LVO and 1.0 wt.% MP-coated LVO samples (b). The corresponding charge/discharge profiles of the bare LVO (c) and 1.0 wt% MP-coated LVO (d) samples originating from Figure 5b. The long-term rate properties of the bare LVO (e) and 1.0 wt% MP-coated LVO (f) samples. Reprint with permission [10] © 2018 Wiley-VCH Verlag GmbH & Co. KGaA, Weinheim.

7.4. LiV₃O₈–Conducting Polymer Composites by RPR Method and the Research Gap

The coating of conducting polymers or LiV₃O₈/conducting polymer composites is favorable in terms of electronic conduction, and hence enhances the electrochemical performance of the material (Table 2). Feng CQ et al. [22] prepared conductive polypyrrole (PPy) via oxidative chemical polymerization technique and the 15 and 20 wt% PPy added-LiV₃O₈ composite was prepared by simple dispersion of LVO and PPy in ethanol through ultrasound bath and the composite powder. Sau et al. [35] used in situ oxidative polymerization method to prepare PPy-LiV₃O₈ composite with LiV₃O₈ (1g), 0.038 mol dm⁻³ pyrrole, 0.013 mol dm⁻³ of sodium p-toluenesulfonate (PTSNa) as the dopant and ferric trichloride (FeCl₃) as the oxidant. Li W et al. [68] prepared (14, 17, and 33 wt%) PTPAN-LiV₃O₈ composites using an in situ chemical polymerization method. LiV₃O₈ (0.2 g), TPA monomer (0.04 g) (0.162 mmol, 20 wt% PTPAN content), chloroform (CHCl₃) (50 mL), and 0.648 mmol FeCl₃ as oxidant were used to synthesize LiV₃O₈-PTPAN composites. Zhu

L et al. [69] synthesized (10, 20, 30, and 40 wt%) PEDOT - LiV_3O_8 composites using an in situ polymerization method. Certain amounts of 3, 4-ethylenedioxythiophene (EDOT) monomer, LiV_3O_8 , CHCl_3 (50 mL), and, FeCl_3 (4:1, $\text{FeCl}_3/\text{EDOT}$ mole ratio) were used for the composite preparation. In the same way, Zhu L et al. [70] prepared $\text{LiV}_3\text{O}_8/\text{PDPA}$ (5, 10, 20, and 30 wt%) nanocomposites where the monomer diphenylamine (DPA) was used in place of EDOT. All the above composites were prepared by the RPR method. Although the conducting polymers enhance the electronic conduction of LiV_3O_8 , all the above materials involve the preparation of conducting polymers which are very complex in nature and add extra cost to the material. We suggest the in situ preparation of carbon-coated LiV_3O_8 by RPR methods, which are yet to be explored by researchers.

When the LiV_3O_8 /conducting polymer composites are synthesized, the conducting polymers perform both binding and conducting functions which replace and reduce the inert weight of carbon black and binders [22]. Production of more diffusion paths for Li^+ intercalation, lower electrochemical polarization of the composite electrode, suppressed phase transition, and decreases in the inter-particle contact resistance are the main reasons for the notable performance by LVO-conducting polymer composites [22,35,68–70]. For example, Zhu L et al. [70] proposed a 10 wt% LiV_3O_8 /PDPA composite which showed an initial charge/discharge capacity of 311 mAh/g whereas it was only 286 mAh/g for bare LiV_3O_8 . After 50 cycles the capacity retention was 272 and 169 mAh/g for 10 wt% LiV_3O_8 /PDPA composite and bare LiV_3O_8 respectively. It is seen that even at a high current density of 2000 mA g^{-1} it shows good discharge capacity. Figure 10 shows the schematic illustrations of Li^+ and electron transfer pathways for LVO and LVO/PDPA composites.

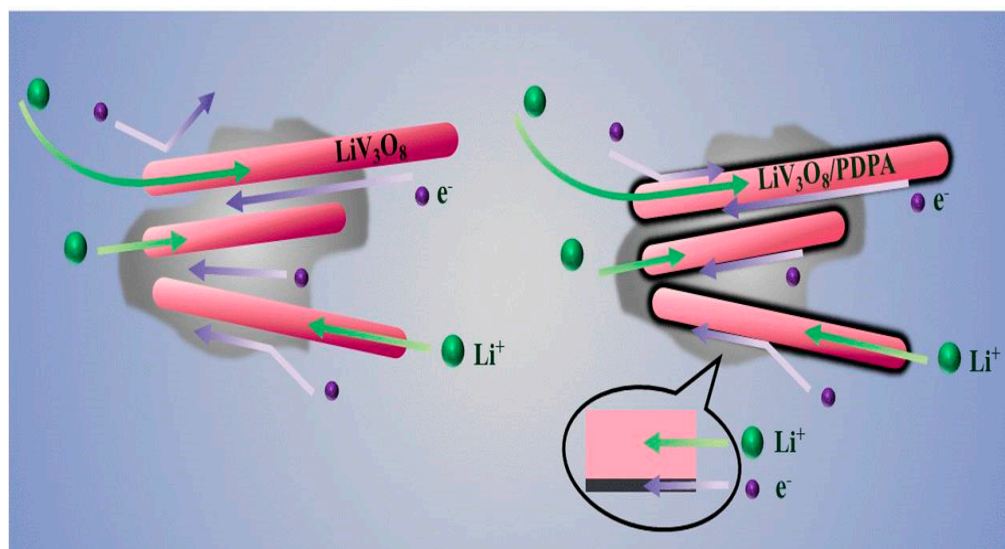


Figure 10. Schematic illustration of Li^+ and electron transfer pathway for LVO and LVO/PDPA composites Reprint with permission [70] © 2018 American Chemical Society.

The decomposition temperature and the weight loss of polymer in the composites were examined for composites LiV_3O_8 -PPy [35], LiV_3O_8 -PTPAn [68], and LiV_3O_8 -PEDOT [69]. PPy showed a single step weight loss at 600°C and 24 wt% PPy was found in PPy- LiV_3O_8 composite [35]. PTPAn began to decompose at 450°C and had a complete breakdown at 800°C which led to only 14, 17 and 33 wt% from 20, 30, and 40 wt% of the PTPAn content in the PTPAn- LiV_3O_8 composites. In the case of PEDOT, the degradation was between 240 – 400°C [69]. This exhibited the approximate weight contents of 10, 20, 30, and 40 wt% LVO/PEDOT composites to be 8, 18, 28, and 37 wt% PEDOT respectively. From this, it can be seen that only PEDOT shows less decomposition at low temperatures and the weight loss is found to be less. In this regard, the in situ carbon coating on LiV_3O_8 by the RPR method under inert atmospheres is most favorable rather than relying on the conducting polymers. Since this cathode material has potential applications in high

temperature polymer battery applications, the decomposition of conducting polymers are high temperature and the operation may be detrimental to the battery performance.

Hence, the major drawback associated with this approach is the thermal decomposition of the conducting polymers, which needs to be addressed by in situ doping with carbon with the Green RPR method approach. The RPR method under an inert atmosphere has been effectively utilized to prepare carbon coated cathode materials for energy applications, with no problem with thermal decomposition as observed in the case of conducting polymer-added LiV_3O_8 .

Hence, further investigations on the change in atmosphere gas to retain the carbon contents on LiV_3O_8 have to be considered. The making of LiV_3O_8 in an argon atmosphere will enhance its electronic properties and in turn improve its electrochemical performance.

8. Preparation of Electrolyte by RPR Method for LIB

The RPR method was not only utilized for the making of metal oxides as anodes and cathodes, but also the preparation of electrolytes such as lithium bis(oxalate) borate (LiBOB) for lithium battery applications [79]. One of the reports shows this method to be more suitable for the making of NASICON type $\text{Li}_{1.4}\text{Al}_{0.4}\text{Ge}_{0.2}\text{Ti}_{1.4}(\text{PO}_4)_3$ solid electrolyte, which shows a higher ionic conductivity of 4.35 mS/cm for battery applications [80]. The authors emphasized that the RPR method is more suitable for the making of the above solid electrolyte than the solid-state method or liquid-phase methods as proved by their report.

9. Materials Other Than Metal Oxides by RPR Method for Various Applications

Apart from the preparation of metal oxides for lithium ion battery applications, the RPR method is also used for the preparation of other materials and other applications as in the following reports. Jing J et al. [81] have reported on the structural and magnetic properties of Gd-Doped Li-Ni Ferrites, $\text{LiNi}_{0.5}\text{Gd}_x\text{Fe}_{2-x}\text{O}_4$ by the RPR method. The authors have successfully made phase-pure Gd-doped ferrites by the RPR method in the range of $x = 0-0.4$, with spherical particles of size about 100 nm. The authors reported the materials to give good magnetic properties. The authors also reported on the preparation and magnetic properties of nanocrystalline Zn-Cu-Cr-Sm ferrite by the RPR method [82]. Zhou X et al. [83] reported on the preparation and magnetic properties of La-substituted Zn-Cu-Cr ferrites by the RPR method and studied its magnetic properties. Cong C. J. et al. [84] reported on the ferromagnetic properties of Mn-doped ZnO nanoparticles prepared by the RPR method and reported it to be an important method of preparing ZnO as a nanosized diluted magnetic semiconductor. Y. Cheng et al. [85] synthesized sodium carboxymethyl cellulose (NaCMC)-stabilized nano zero-valent iron (C-nZVI) by RPR method to study the decolorization of reactive blue-19 dye. A high decolorization efficiency of 94.5% was achieved within 30 min with a removal rate constant was 0.0447 min^{-1} . X. Han et al. [86] synthesized metal-organic complexes of rufigallol-Li/Ni complex (R-LN) by the RPR method. A high yield of the complex was obtained and tested as an anode material for LIB. J. Sun et al. synthesized [87] Tb^{3+} -doped zinc salicylate, $\text{Zn}(\text{HOC}_6\text{H}_4\text{CO}_2)_2:\text{Tb}$ by RPR method. J. Sun et al. [88] synthesized zinc phthalate using the RPR method and its thermal decomposition reaction mechanism is investigated in an inert atmosphere. J. Yao et al. [89] synthesized $\text{Ni}_{0.9}\text{Mn}_{2.1-x}\text{Mg}_x\text{O}_4$ ($0 \leq x \leq 0.3$) negative temperature coefficient (NTC) material. The authors synthesized using different compositions using MnO_2 , Ni_2O_3 , MgO , and $\text{H}_2\text{C}_2\text{O}_4 \cdot 2\text{H}_2\text{O}$ and proved that RPR is a promising technique for the synthesis of $\text{Ni}_{0.9}\text{Mn}_{2.1-x}\text{Mg}_x\text{O}_4$ NTC ceramic materials.

10. Limitations of the RPR Method

When designing a reaction using the RPR method, careful consideration should be given to the following factors: (1) the mixture of the reactants, the ratio of the reactants, the solvent selection, and the quantity of reaction byproducts that have been separated; (2) the mixing process, time, pace, and flow of the system; and (3) the heating time and temperature of the precursors.

11. Conclusions

The utilization of the rheological phase reaction (RPR) method for the preparation of various metal oxides and electrolytes for LIB applications is discussed in detail, which proved the RPR method is an industrial method to be adopted for making materials to develop high efficiency energy devices. The critical review of the structural and morphology changes, and electrochemical properties of LiV_3O_8 prepared by the RPR method shows a higher specific capacity of the material for a low calcination temperature of 400–500 °C. Modifying LiV_3O_8 prepared by the RPR method via doping, coating, and compositing with suitable materials such as hetero-atoms, metal oxides, and conducting polymers has a significant effect on the electrochemical properties. They hinder the fast capacity decay during charge and discharge processes, growth of dendrite, and dissolution of LiV_3O_8 into the electrolyte by avoiding the direct contact between the electrode and electrolyte. From this, it can be concluded that LiV_3O_8 prepared by the RPR method is more efficient for battery applications. Apart from a metal oxide, this method is found to be suitable for the preparation of phase-pure nanoparticles of any material. The RPR method is proven to be the best for the preparation of metal oxide/carbon composites. It has been discovered that the RPR approach makes it inexpensive and simple to commercialize new materials. This method makes it feasible to produce materials on a large scale, which lowers the overall cost of the finished goods. Additionally, there is no requirement for the costly and harmful inorganic solvents. The RPR method is an effective approach for the synthesis of materials and their commercialization because of its uncomplicated reaction steps, inexpensive reactants, and high yield of products. Overall, the RPR method stands out as the pollution-less mass production approach among the various other preparation routes and hence more research work is to be carried out in utilizing the benefits of this method.

Author Contributions: Conceptualization, methodology, writing—original draft preparation—S.P. Validation, writing—review and editing, visualization, supervision—A.S., M.V.V.R. Project administration, funding acquisition—A.S. All authors have read and agreed to the published version of the manuscript.

Funding: Department of Science and Technology, Science and Engineering Research Board, (DST-SERB), Project No. EMR/2017/003227 dated 16th July 2018.

Institutional Review Board Statement: Not applicable.

Informed Consent Statement: Not applicable.

Data Availability Statement: Not applicable.

Acknowledgments: The authors thank the Department of Science and Technology, Science and Engineering Research Board, (DST-SERB) for the financial assistance through Project No. EMR/2017/003227 dated 16 July 2018.

Conflicts of Interest: The authors declare no conflict of interest.

References

1. Dhas, S.; Maldar, P.; Patil, M.; Waikar, M.; Sonkawade, R.; Moholkar, A.V. Sol-gel synthesized nickel oxide nanostructures on nickel foam and nickel mesh for a targeted energy storage application. *J. Energy Storage* **2022**, *47*, 103658. [[CrossRef](#)]
2. Yewale, M.; Jadhavar, A.; Kadam, R.; Velhal, N.; Nakate, U.; Teli, A.; Shin, J.; Nguyen, L.; Shin, D.; Kaushik, N. Hydrothermal synthesis of manganese oxide (Mn_3O_4) with granule-like morphology for supercapacitor application. *Ceram. Int.* **2022**, *48*, 29429–29437. [[CrossRef](#)]
3. Manafi, S.; Tazikeh, S.; Joughehdoust, S. Synthesis and characterization of indium tin oxide nanoparticles via reflux method. *Mater. Sci. Pol.* **2017**, *35*, 799–805. [[CrossRef](#)]
4. Palem, R.; Shimoga, G.; Rabani, I.; Bathula, C.; Seo, Y.-S.; Kim, H.-S.; Kim, S.-Y.; Lee, S.-H. Ball-milling route to design hierarchical nanohybrid cobalt oxide structures with cellulose nanocrystals interface for supercapacitors. *Int. J. Energy Res.* **2022**, *46*, 8398–8412. [[CrossRef](#)]
5. Rajput, A.; Sharma, P.; Yadav, V.; Gupta, H.; Kulshrestha, V. Synthesis and characterization of different metal oxide and GO composites for removal of toxic metal ions. *Sep. Sci. Technol.* **2019**, *54*, 426–433. [[CrossRef](#)]

6. Sumantha, H.; Rajagopal, S.; Shashank, M.; Nagaraju, G.; Pattar, V.; Shanmugaraj, P.; Ayyasamy, S.; Suresha, B. Green synthesis and characterization of Mn_3O_4 nanoparticles for photocatalytic and supercapacitors. *Ionics* **2022**. [[CrossRef](#)]
7. Veena, B.; Pavithra, S.; Seetha, M. Cr doped CeO_2 nanoparticles as supercapacitor electrodes Cr doped CeO_2 nanoparticles as supercapacitor electrodes. *AIP Adv.* **2022**, *12*, 125310. [[CrossRef](#)]
8. Chen, X.; Zhang, Z.; Fang, J.; Zhang, Y.; Zhao, C.; Wu, Y.; Li, W. TiO_2 nanoparticles via simple surface modification as cathode interlayer for efficient organic solar cells. *Org. Electron.* **2022**, *101*, 106422. [[CrossRef](#)]
9. Eng, J.; Bensalah, N.; Dawood, H. Review on Synthesis, Characterizations, and Electrochemical Properties of Cathode Materials for Lithium Ion Batteries. *J. Mater. Sci. Eng.* **2016**, *5*. [[CrossRef](#)]
10. Xie, L.; Ge, P.; Zhu, L.; Cao, X. Stabilization of LiV_3O_8 Rod-like Structure by Protective $Mg_3(PO_4)_2$ Layer for Advanced Lithium Storage Cathodes. *Energy Technol.* **2018**, *6*, 2479–2487. [[CrossRef](#)]
11. Ying, J.; Jiang, C.; Wan, C. Preparation and characterization of high-density spherical $LiCoO_2$ cathode material for lithium ion batteries. *J. Power Sources* **2004**, *129*, 264–269. [[CrossRef](#)]
12. Xu, H.; Sun, J.; Gao, L. Hydrothermal synthesis of $LiMnO_2$ microcubes for lithium ion battery application. *Ionics* **2013**, *19*, 63–69. [[CrossRef](#)]
13. Huang, X.; Ma, J.; Wu, P.; Hu, Y.; Dai, J.; Zhu, Z.; Chen, H.; Wang, H. Hydrothermal synthesis of $LiCoPO_4$ cathode materials for rechargeable lithium ion batteries. *Mater. Lett.* **2005**, *59*, 578–582. [[CrossRef](#)]
14. Kim, D.; Muralidharan, P.; Lee, H.; Ruffo, R.; Chan, C.; Peng, H.; Huggins, R.; Cui, Y.; Kim, D.; Muralidharan, P.; et al. Spinel $LiMn_2O_4$ Nanorods as Lithium Ion Battery Cathodes. *Nano Lett.* **2008**, *8*, 3948–3952. [[CrossRef](#)] [[PubMed](#)]
15. Wang, G.; Zhong, S.; Bradhurst, D.; Dou, S.; Liu, H. Synthesis and characterization of $LiNiO_2$ compounds as cathodes for rechargeable lithium batteries. *J. Power Sources* **1998**, *76*, 141–146. [[CrossRef](#)]
16. Higuchi, M.; Katayama, K.; Azuma, Y. Synthesis of $LiFePO_4$ cathode material by microwave processing. *J. Power Sources* **2003**, *121*, 258–261. [[CrossRef](#)]
17. Abouimrane, A.; Armand, M. Electrochemical performance of Li_2FeSiO_4 as a new Li-battery cathode material. *Electrochem. Commun.* **2005**, *7*, 156–160. [[CrossRef](#)]
18. Gaubicher, J.; Wurm, C.; Goward, G. Rhombohedral Form of $Li_3V_2(PO_4)_3$ as a Cathode in Li-Ion Batteries. *Chem. Mater.* **2000**, *2*, 3240–3242. [[CrossRef](#)]
19. Wu, W.; Ding, J.; Peng, H.; Li, G. Synthesis and electrochemical properties of single-crystalline LiV_3O_8 nanobelts for rechargeable lithium batteries. *Mater. Lett.* **2011**, *65*, 2155–2157. [[CrossRef](#)]
20. Liu, X.; Wang, J.; Zhang, J.; Yang, S. Sol–gel template synthesis of LiV_3O_8 nanowires. *J. Mater. Sci.* **2007**, *42*, 867–871. [[CrossRef](#)]
21. Yan, H.; Wang, H.; Qiang, Z. Novel chemical method for synthesis of LiV_3O_8 nanorods as cathode materials for lithium ion batteries. *Electrochim. Acta* **2004**, *49*, 349–353. [[CrossRef](#)]
22. Feng, C.; Chew, S.; Guo, Z.; Wang, J.; Liu, H. An investigation of polypyrrole— LiV_3O_8 composite cathode materials for lithium-ion batteries. *J. Power Sources* **2007**, *174*, 1095–1099. [[CrossRef](#)]
23. Kumagai, N. Ultrasonically Treated LiV_3O_8 as a Cathode Material for Secondary Lithium Batteries. *J. Electrochem. Soc.* **1997**, *144*, 830. [[CrossRef](#)]
24. Huang, S.; Lu, Y.; Wang, T.; Gu, C.; Wang, X.; Tu, J. Polyacrylamide-assisted freeze drying synthesis of hierarchical plate-arrayed LiV_3O_8 for high-rate lithium-ion batteries. *J. Power Sources* **2013**, *235*, 256–264. [[CrossRef](#)]
25. Wu, F.; Wang, L.; Wu, C.; Bai, Y.; Wang, F. Study on $Li_{1+x}V_3O_8$ synthesized by microwave sol–gel route. *Mater. Chem. Phys.* **2009**, *115*, 707–711. [[CrossRef](#)]
26. Ju, S.; Kang, Y. Electrochimica Acta Morphological and electrochemical properties of LiV_3O_8 cathode powders prepared by spray pyrolysis. *Electrochim. Acta* **2010**, *55*, 6088–6092. [[CrossRef](#)]
27. Fang, D.; Cui, M.; Bao, R.; Yi, J.; Luo, Z. In-situ coating polypyrrole on charged $BiVO_4$ nanowire arrays to improve lithium-ion storage properties. *Solid State Ionics* **2020**, *346*, 115222. [[CrossRef](#)]
28. Scientific, C. Crystal chemistry of non-stoichiometric pentavalent vanadium oxides: Crystal structure of $Li_{1+x}V_3O_8$. *Acta Crystallogr.* **1957**, *10*, 261–267. [[CrossRef](#)]
29. Pistoia, G.; Wang, G.; Zane, D. Mixed Na/K vanadates for rechargeable Li batteries. *Solid State Ionics* **1995**, *76*, 285–290. [[CrossRef](#)]
30. Feng, Y.; Li, Y.; Hou, F. Preparation and electrochemical properties of Cr doped LiV_3O_8 cathode for lithium ion batteries. *Mater. Lett.* **2009**, *63*, 1338–1340. [[CrossRef](#)]
31. Song, H.; Liu, Y.; Zhang, C.; Liu, C.; Cao, G. Mo-doped LiV_3O_8 nanorod-assembled nanosheets as a high performance cathode material for lithium ion batteries. *J. Mater. Chem. A* **2015**, *3*, 3547–3558. [[CrossRef](#)]
32. Jiao, L.; Li, H.; Yuan, H.; Wang, Y. Preparation of copper-doped LiV_3O_8 composite by a simple addition of the doping metal as cathode materials for lithium-ion batteries. *Mater. Lett.* **2008**, *62*, 3937–3939. [[CrossRef](#)]
33. Zhao, M.; Jiao, L.; Yuan, H.; Feng, Y.; Zhang, M. Study on the silicon doped lithium trivanadate as cathode material for rechargeable lithium batteries. *Solid State Ionics* **2007**, *178*, 387–391. [[CrossRef](#)]
34. Feng, Y.; Li, Y.; Hou, F. Boron doped lithium trivanadate as a cathode material for an enhanced rechargeable lithium ion batteries. *J. Power Sources* **2009**, *187*, 224–228. [[CrossRef](#)]
35. Fang, H.; Mo-ran, S.; Yu-sheng, W.; Chun-hua, Z. The synthesis and electrochemical performance of LiV_3O_8 cathode with Lanthanum-doped. *Adv. Mater. Res.* **2012**, *1*, 860–863. [[CrossRef](#)]

36. Ng, S. Low-temperature synthesis of polypyrrole-coated LiV_3O_8 composite with enhanced electrochemical properties. *J. Electrochem. Soc.* **2007**, *154*, 3–9.
37. Liu, Q.; Liu, H.; Zhou, X.; Cong, C.; Zhang, K. A soft chemistry synthesis and electrochemical properties of LiV_3O_8 as cathode material for lithium secondary batteries. *Solid State Ionics* **2005**, *176*, 1549–1554. [[CrossRef](#)]
38. Qiao, Y.; Wang, X.; Zhou, J.; Zhang, J.; Gu, C.; Tu, J. Synthesis and electrochemical performance of rod-like LiV_3O_8 cathode materials for rechargeable lithium batteries. *J. Power Sources* **2012**, *198*, 287–293. [[CrossRef](#)]
39. Daniel, C.; Mohanty, D.; Li, J.; Wood, D.; Daniel, C.; Mohanty, D.; Li, J.; Wood, D. Cathode materials review. *AIP Conf. Proc.* **2015**, *1597*, 26. [[CrossRef](#)]
40. Xu, B.; Qian, D.; Wang, Z.; Meng, Y. Recent progress in cathode materials research for advanced lithium ion batteries. *Mater. Sci. Eng. R Rep.* **2012**, *73*, 51–65. [[CrossRef](#)]
41. Kraysberg, A.; Ein-eli, Y. Higher, Stronger, Better ... A Review of 5 Volt Cathode Materials for Advanced Lithium-Ion Batteries. *Adv. Energy Mater.* **2012**, *2*, 922–939. [[CrossRef](#)]
42. Mai, L.; Xu, X.; Xu, L.; Han, C.; Luo, Y. Vanadium oxide nanowires for Li-ion batteries. *J. Mater. Res.* **2011**, *26*, 2175–2185. [[CrossRef](#)]
43. Shi, X.; Xiao, Y.; Li, M.; Yuan, L.; Sun, J. Synthesis of an industrially important zinc borate, $2\text{ZnO} \cdot 3\text{B}_2\text{O}_3 \cdot 3\text{H}_2\text{O}$, by a rheological phase reaction method. *Powder Technol.* **2008**, *186*, 263–266. [[CrossRef](#)]
44. Lee, S.; Kim, H.; Kim, M.; Youn, H.; Kang, K.; Cho, B.; Roh, K.; Kim, K. Improved electrochemical performance of $\text{LiNi}_{0.6}\text{Co}_{0.2}\text{Mn}_{0.2}\text{O}_2$ cathode material synthesized by citric acid assisted sol-gel method for lithium ion batterie. *J. Power Sources* **2016**, *315*, 261–268. [[CrossRef](#)]
45. Zhang, Y.; Cao, H.; Zhang, J.; Xia, B. Synthesis of $\text{LiNi}_{0.6}\text{Co}_{0.2}\text{Mn}_{0.2}\text{O}_2$ cathode material by a carbonate co-precipitation method and its electrochemical characterization. *Solid State Ionics* **2006**, *177*, 3303–3307. [[CrossRef](#)]
46. Jo, C.-H.; Cho, D.-H.; Noh, H.-J.; Yashiro, H.; Sun, Y.-K.; Myung, S. An effective method to reduce residual lithium compounds on Ni-rich $\text{Li}[\text{Ni}_{0.6}\text{Co}_{0.2}\text{Mn}_{0.2}]\text{O}_2$ active material using a phosphoric acid derived Li_3PO_4 nanolayer. *Nano Res.* **2015**, *8*, 1464–1479. [[CrossRef](#)]
47. Noh, H.-J.; Youn, S.; Yoon, C.; Sun, Y.-K. Comparison of the structural and electrochemical properties of layered $\text{Li}[\text{Ni}_x\text{Co}_y\text{Mn}_z]\text{O}_2$ ($x = 1/3, 0.5, 0.6, 0.7, 0.8$ and 0.85) cathode material for lithium-ion batteries. *J. Power Sources* **2013**, *233*, 121–130. [[CrossRef](#)]
48. Zhong, S.; Li, W.; Zuo, Z.; Tang, X.; Li, Y. Synthesis and electrochemical performances of $\text{LiNi}_{0.6}\text{Co}_{0.2}\text{Mn}_{0.2}\text{O}_2$ cathode materials. *Trans. Nonferrous Met. Soc. China* **2009**, *19*, 1499–1503. [[CrossRef](#)]
49. Ju, S.; Kang, I.-S.; Lee, Y.-S.; Shin, W.-K.; Kim, S.; Shin, K.; Kim, D.-W. Improvement of the Cycling Performance of $\text{LiNi}_{0.6}\text{Co}_{0.2}\text{Mn}_{0.2}\text{O}_2$ Cathode Active Materials by a Dual-Conductive Polymer Coating. *ACS Appl. Mater. Interfaces* **2014**, *6*, 2546–2552. [[CrossRef](#)]
50. Xie, T.; Sun, F.; Zhou, X.; Liu, L.; Liu, Z.; Liu, L.; Wu, Z.; Yue, Z.; Zhou, L.; Tang, H. Rheological phase method synthesis of carbon-coated $\text{LiNi}_{0.6}\text{Co}_{0.2}\text{Mn}_{0.2}\text{O}_2$ as the cathode material of high-performance lithium-ion batteries. *Appl. Phys. A* **2018**, *124*, 720. [[CrossRef](#)]
51. Wang, W.; Wang, H.; Yu, Y.; Wu, Z.; Asif, M.; Liu, H. Metallic cobalt modified $\text{MnO}-\text{C}$ nanocrystalline composites as an efficient bifunctional oxygen electrocatalyst. *Catal. Sci. Technol.* **2018**, *8*, 480–485. [[CrossRef](#)]
52. Liu, H.; Luo, S.; Hu, D.; Liu, X.; Wang, Q.; Wang, Z.; Wang, Y.; Chang, L.; Liu, Y.; Yi, T.-F.; et al. Design and synthesis of carbon-coated $\alpha\text{-Fe}_2\text{O}_3@ \text{Fe}_3\text{O}_4$ heterostructured as anode materials for lithium ion batteries. *Appl. Surf. Sci.* **2019**, *495*, 143590. [[CrossRef](#)]
53. Cao, X.; Yang, Q.; Zhu, L.; Xie, L. NaV_3O_8 with superior rate capability and cycle stability as cathode materials for sodium-ion batteries. *Ionics* **2018**, *24*, 943–949. [[CrossRef](#)]
54. Yin, S.; Song, L.; Wang, X.; Zhang, M.; Zhang, K.; Zhang, Y. Synthesis of spinel $\text{Li}_4\text{Ti}_5\text{O}_{12}$ anode material by a modified rheological phase reaction. *Electrochim. Acta* **2009**, *54*, 5629–5633. [[CrossRef](#)]
55. Shi, X.; Wang, C.; Zhang, Y.; Liu, Q.; Li, H.; Song, D.; Zhang, L. Structure and electrochemical behaviors of spherical $\text{Li}_{1+x}\text{Ni}_{0.5}\text{Mn}_{0.5}\text{O}_{2+\delta}$ synthesized by rheological phase reaction method. *Electrochim. Acta* **2014**, *150*, 89–98. [[CrossRef](#)]
56. Yan, J.; Wang, P.; Fang, H.; Wang, L.-X.; Li, L.; Gao, H.-L.; Wang, L.-Z.; Zhang, L.-S.; Song, Y.-H.; Tang, Z.-Y. Enhanced rate performance of $\text{Li}_3\text{V}_2(\text{PO}_4)_3/\text{C}$ cathode by an improved rheological phase assisted microwave method. *Mater. Res. Bull.* **2018**, *106*, 250–256. [[CrossRef](#)]
57. Liu, H.; Liu, L.; Ding, C. A quick microwave-assisted rheological phase reaction route for preparing $\text{Cu}_3\text{Mo}_2\text{O}_9$ with excellent lithium storage and supercapacitor performance. *J. Alloys Compd.* **2021**, *867*, 159061. [[CrossRef](#)]
58. Shi, X.; Chang, C.; Xiang, J.; Xiao, Y.; Yuan, L.; Sun, J. Synthesis of nanospherical Fe_3BO_6 anode material for lithium-ion battery by the rheological phase reaction method. *J. Solid State Chem.* **2008**, *181*, 2231–2236. [[CrossRef](#)]
59. Peng, H.; Zhu, Z.; Huang, P.; Li, X. Effects of Synthesis Temperature and Holding Time on the Electrochemical Properties of $\text{LiNi}_{1/3}\text{Co}_{1/3}\text{Mn}_{1/3}\text{O}_2$ Cathode Material Using Rheological Phase Method. *Mater. Sci. Forum.* **2015**, *814*, 351–357. [[CrossRef](#)]
60. Huang, X.; Hu, Q.; Liu, J.; Liu, H. Submicron Li_2MoO_4 material prepared by rheological phase method and its evaluation of lithium storage performances. *Ionics* **2017**, *23*, 2269–2273. [[CrossRef](#)]
61. Zheng, H.; Wang, T.; Zhao, R.; Chen, J.; Li, L. Cryptomelane-type manganese oxide ($\text{KMn}_8\text{O}_{16}$) nanorods cathode materials synthesized by a rheological phase for lithium ion batteries. *IOP Conf. Ser. Earth Environ. Sci.* **2018**, *108*, 022012. [[CrossRef](#)]

62. Li, Y.; Xu, G.; Fan, S.; Ma, J.; Shi, X.; Long, Z.; Deng, W.; Fan, W.; Yang, S. Synthesis of carbon-coated $\text{LiMn}_{0.8}\text{Fe}_{0.2}\text{PO}_4$ materials via an aqueous rheological phase-assisted solid-state method. *J. Solid State Electrochem.* **2020**, *24*, 821–828. [[CrossRef](#)]
63. Wu, Y.; Tang, Z.; Guo, X.; Du, C.; Zhang, X. An alginate acid assisted rheological phase synthesis of carbon coated $\text{Li}_3\text{V}_2(\text{PO}_4)_3$ with high-rate performance. *J. Alloys Compd.* **2014**, *616*, 32–41. [[CrossRef](#)]
64. Zhong, Y.-J.; Li, J.-T.; Wu, Z.-G.; Guo, X.-D.; Zhong, B.-H.; Sun, S.-G. $\text{LiMn}_{0.5}\text{Fe}_{0.5}\text{PO}_4$ solid solution materials synthesized by rheological phase reaction and their excellent electrochemical performances as cathode of lithium ion battery. *J. Power Sources* **2013**, *234*, 217–222. [[CrossRef](#)]
65. Hu, Y.; Liu, X. A novel method for preparing $\alpha\text{-LiFeO}_2$ nanorods for high-performance lithium-ion batteries. *Ionics* **2020**, *26*, 1057–1061. [[CrossRef](#)]
66. Cao, X.; Guo, L.; Liu, J.; Xie, L. Preparation of ZnO-Coated LiV_3O_8 as Cathode Materials for Rechargeable Lithium Batteries. *Int. J. Electrochem. Sci.* **2011**, *6*, e278.
67. Xie, L.; Xu, Y.; Zhang, J.; Zhang, C.; Cao, X.; Qu, L. Rheological Phase Synthesis of Er-Doped LiV_3O_8 as Electroactive Material for a Cathode of Secondary Lithium Storage. *Electron. Mater. Lett.* **2013**, *9*, 549–553. [[CrossRef](#)]
68. Li, W.; Zhu, L.; Yu, Z.; Xie, L.; Cao, X. Enhanced Electrochemical Performances as Cathode. *Materials* **2017**, *10*, 344. [[CrossRef](#)]
69. Zhu, L.; Li, W.; Yu, Z.; Xie, L.; Cao, X. Synthesis and electrochemical performances of $\text{LiV}_3\text{O}_8/\text{poly}(3,4\text{-ethylenedioxythiophene})$ composites as cathode materials for rechargeable lithium batteries. *Solid State Ionics* **2017**, *310*, 30–37. [[CrossRef](#)]
70. Zhu, L.; Xie, L.; Cao, X. Energy, Environmental, and Catalysis Applications $\text{LiV}_3\text{O}_8/\text{Polydiphenylamine}$ Composites with Significantly Improved Electrochemical Behavior as Cathode Materials for Rechargeable Lithium Batteries. *ACS Appl. Mater. Interfaces* **2018**, *10*, 10909–10917. [[CrossRef](#)] [[PubMed](#)]
71. Zhang, H.; Neilson, J.; Morse, D. Vapor-Diffusion-Controlled Sol-Gel Synthesis of Flaky Lithium Vanadium Oxide and Its Electrochemical Behavior. *J. Phys. Chem. C* **2010**, *8*, 19550–19555. [[CrossRef](#)]
72. Liu, H.; Novák, P. Electrochemistry of LiV_3O_8 Nanoparticles Made by Flame spray pyrolysis. *Electrochem. Solid-State Lett.* **2008**, *11*, 46–50. [[CrossRef](#)]
73. Zhou, Y.; Yue, H.; Zhang, X.; Deng, X. Preparation and characterization of LiV_3O_8 cathode material for lithium secondary batteries through an EDTA-sol-gel method. *Solid State Ionics* **2008**, *179*, 1763–1767. [[CrossRef](#)]
74. Tran, N.; Bramnik, K.; Hibst, H.; Pröhl, J.; Mronga, N.; Holzapfel, M.; Scheifele, W.; Novák, P. Spray-Drying Synthesis and Electrochemical Performance of Lithium Vanadates as Positive Electrode Materials for Lithium Batteries. *J. Electrochem. Soc.* **2008**, *155*, 384–389. [[CrossRef](#)]
75. Cui, P.; Jia, Z.; Li, L.; He, T. Study on the performance characteristics of Li–V–O nanocomposite as cathode material for Li-ion batteries. *Electrochim. Acta* **2011**, *56*, 4571–4575. [[CrossRef](#)]
76. Kim, B.; Bae, K.; Cho, S.; Yoon, W. Electrochemical Behaviors of a Vapor-Phase Polymerized Conductive Polymer Coated on LiV_3O_8 in Li–Metal Rechargeable Batteries. *ACS Appl. Mater. Interfaces* **2018**, *10*, 28695–28701. [[CrossRef](#)] [[PubMed](#)]
77. Cao, X.; Zhu, L.; Wu, H. Preparation and Electrochemical Performances of Rod-Like $\text{LiV}_3\text{O}_8/\text{Carbon}$ Composites Using Polyaniline as Carbon Source. *Electron. Mater. Lett.* **2015**, *11*, 650–657. [[CrossRef](#)]
78. Yang, G.; Hou, W.; Sun, Z.; Yan, Q. A novel inorganic–Organic polymer electrolyte with a high conductivity: Insertion of poly(ethylene) oxide into LiV_3O_8 in one step. *J. Mater. Chem.* **2005**, 1369–1374. [[CrossRef](#)]
79. Lian, F.; Li, Y.; He, Y.; Guan, H.; Yan, K.; Qiu, W.; Chou, K.-C.; Axmann, P.; Wohlfahrt-Mehrens, M. Preparation of LiBOB via rheological phase method and its application to mitigate voltage fade of $\text{Li}_{1.16}[\text{Mn}_{0.75}\text{Ni}_{0.25}]_{0.84}\text{O}_2$ cathode. *RSC Adv.* **2015**, *5*, 86763–86770. [[CrossRef](#)]
80. Bai, F.; Kakimoto, K.; Shang, X.; Mori, D.; Taminato, S.; Matsumoto, M.; Takeda, Y.; Yamamoto, O.; Minami, H.; Izumi, H.; et al. Synthesis of NASICON type $\text{Li}_{1.4}\text{Al}_{0.4}\text{Ge}_{0.2}\text{Ti}_{1.4}(\text{PO}_4)_3$ solid electrolyte by rheological phase method. *J. Asian Ceram. Soc.* **2020**, *8*, 476–483. [[CrossRef](#)]
81. Jing, J.; Liangchao, L.; Feng, X. Structural Analysis and Magnetic Properties of Gd-Doped Li–Ni Ferrites Prepared Using Rheological Phase Reaction Method. *J. Rare Earths* **2007**, *25*, 79–83. [[CrossRef](#)]
82. Jiang, J.; Li, L.; Xu, F.; Xie, Y. Preparation and magnetic properties of Zn–Cu–Cr–Sm ferrite via a rheological phase reaction method. *Mater. Sci. Eng. B* **2007**, *137*, 166–169. [[CrossRef](#)]
83. Zhou, X.; Jiang, J.; Li, L.; Xu, F. Preparation and magnetic properties of La-substituted Zn–Cu–Cr ferrites via a rheological phase reaction method. *J. Magn. Magn. Mater.* **2007**, *314*, 7–10. [[CrossRef](#)]
84. Cong, C.; Liao, L.; Li, J.; Fan, L.; Zhang, K. Synthesis, structure and ferromagnetic properties of Mn-doped ZnO nanoparticles. *Nanotechnology* **2005**, *16*, 981. [[CrossRef](#)]
85. Cheng, Y.; Lu, M.; Jiao, C.; Liu, H.-J. Preparation of stabilized nano zero-valent iron particles via a rheological phase reaction method and their use in dye decolorization. *Environ. Technol.* **2013**, *34*, 445–451. [[CrossRef](#)]
86. Han, X.; Lin, G.; Zhang, Q.; Yang, Y. Rheological phase reaction synthesis and electrochemical performance of rufigallol anode for lithium ion batteries. *RSC Adv.* **2018**, *8*, 19272–19277. [[CrossRef](#)] [[PubMed](#)]
87. Sun, J.; Xie, W.; Yuan, L.; Zhang, K.; Wang, Q. Preparation and luminescence properties of Tb³⁺-doped zinc salicylates. *Mater. Sci. Eng. B Solid-State Mater. Adv. Technol.* **1999**, *64*, 157–160. [[CrossRef](#)]

88. Sun, J.; Yuan, L.; Zhang, K.; Wang, D. Synthesis and thermal decomposition of zinc phthalate. *Thermochim. Acta* **2000**, *343*, 105–109. [[CrossRef](#)]
89. Yao, J.; Zhang, B.; Wang, J.; Chang, A.; Ji, G.; Zhao, P.; Zhao, L. Preparation of $\text{Ni}_{0.9}\text{Mn}_{2.1-x}\text{Mg}_x\text{O}_4$ ($0 \leq x \leq 0.3$) negative temperature coefficient ceramic materials by a rheological phase reaction method. *Mater. Lett.* **2013**, *112*, 69–71. [[CrossRef](#)]

Disclaimer/Publisher's Note: The statements, opinions and data contained in all publications are solely those of the individual author(s) and contributor(s) and not of MDPI and/or the editor(s). MDPI and/or the editor(s) disclaim responsibility for any injury to people or property resulting from any ideas, methods, instructions or products referred to in the content.